

An Inexact Conditional Gradient Method for Constrained Bilevel Optimization

Nazanin Abolfazli* Ruichen Jiang† Aryan Mokhtari† Erfan Yazdandoost Hamedani*

March 18, 2024

Abstract

Bilevel optimization is an important class of optimization problems where one optimization problem is nested within another. While various methods have emerged to address unconstrained general bilevel optimization problems, there has been a noticeable gap in research when it comes to methods tailored for the constrained scenario. The few methods that do accommodate constrained problems, often exhibit slow convergence rates or demand a high computational cost per iteration. To tackle this issue, our paper introduces a novel single-loop projection-free method employing a nested approximation technique. This innovative approach not only boasts an improved per-iteration complexity compared to existing methods but also achieves optimal convergence rate guarantees that match the best-known complexity of projection-free algorithms for solving convex constrained single-level optimization problems. In particular, when the hyper-objective function corresponding to the bilevel problem is convex, our method requires $\tilde{O}(\epsilon^{-1})$ iterations to find an ϵ -optimal solution. Moreover, when the hyper-objective function is non-convex, our method's complexity for finding an ϵ -stationary point is $\mathcal{O}(\epsilon^{-2})$. To showcase the effectiveness of our approach, we present a series of numerical experiments that highlight its superior performance relative to state-of-the-art methods.

1 Introduction

Many learning and inference problems take a *hierarchical* form, where one optimization problem is nested within another. Bilevel optimization is often used to model problems of this kind with two levels of hierarchy. In this paper, we consider the bilevel optimization problem of the form

$$\min_{\mathbf{x} \in \mathcal{X}} \ell(\mathbf{x}) := f(\mathbf{x}, \mathbf{y}^*(\mathbf{x})) \quad \text{s.t. } \mathbf{y}^*(\mathbf{x}) \in \operatorname{argmin}_{\mathbf{y} \in \mathbb{R}^m} g(\mathbf{x}, \mathbf{y}), \quad (1)$$

where $n, m \geq 1$ are integers; $\mathcal{X} \subset \mathbb{R}^n$ is a compact and convex set with diameter $D_{\mathcal{X}}$, i.e., $\|\mathbf{x} - \mathbf{y}\| \leq D_{\mathcal{X}}$ for all $\mathbf{x}, \mathbf{y} \in \mathcal{X}$. Further, $f : \mathcal{X} \times \mathbb{R}^m \rightarrow \mathbb{R}$ and $g : \mathcal{X} \times \mathbb{R}^m \rightarrow \mathbb{R}$ are continuously differentiable functions with respect to \mathbf{x} and \mathbf{y} on an open set containing \mathcal{X} and \mathbb{R}^m , respectively.

*Department of Systems and Industrial Engineering, The University of Arizona, Tucson, AZ, USA
 {nazaninabolfazli@arizona.edu, erfany@arizona.edu}

†Department of Electrical and Computer Engineering, The University of Texas at Austin, Austin, TX, USA
 {rjiang@utexas.edu, mokhtari@austin.utexas.edu}

Problem (1) involves two optimization problems following a two-level structure. The outer objective $f(\mathbf{x}, \mathbf{y}^*(\mathbf{x}))$ depends on \mathbf{x} both directly and also indirectly through $\mathbf{y}^*(\mathbf{x})$, which is a solution of the lower-level problem of minimizing another function g parameterized by \mathbf{x} . Throughout the paper, we assume that $g(\mathbf{x}, \mathbf{y})$ is strongly convex in \mathbf{y} , and hence $\mathbf{y}^*(\mathbf{x})$ is uniquely well-defined for any $\mathbf{x} \in \mathcal{X}$. The application of (1) arises in a number of machine learning problems, such as meta-learning Rajeswaran, Finn, Kakade, and Levine [RFKL19], continual learning Borsos, Mutny, and Krause [BMK20], hyper-parameter optimization [FFSGP18b; Ped16], and data hyper-cleaning Shaban, Cheng, Hatch, and Boots [SCHB19].

Numerous methods have emerged to tackle the general bilevel optimization problems described in (1). For instance, previous works like [HJS92; SLZ05; Moo10] utilized the optimality conditions of the lower-level problem to transform the bilevel problem into a single-level constrained problem. However, this approach faces two significant challenges: (i) The reduced problem becomes excessively constrained when dealing with large-scale inner problems; (ii) Unless the lower-level function g possesses a specific structure, such as a quadratic form, the optimality condition of the lower-level problem introduces nonconvexity into the feasible set of the reduced problem.

Recently, more efficient gradient-based methods for bilevel optimization have emerged, broadly categorized as the approximate implicit differentiation (AID) approach [Ped16; GFCACG16; Dom12; LXFZYPUZ18; GW18; LVD20] and the iterative differentiation (ITD) approach [SCHB19; MDA15; FFSGP18a; GFPS20]. However, except for a few recent efforts that we discuss, most studies have primarily focused on analyzing asymptotic convergence, leaving room for the development of novel algorithms with guaranteed convergence rates.

Moreover, in most previous studies, it is assumed that $\mathcal{X} = \mathbb{R}^n$, simplifying the optimization problem to an unconstrained one. However, several practical applications, such as meta-learning Franceschi, Frasconi, Salzo, Grazzi, and Pontil [FFSGP18b], personalized federated learning Fallah, Mokhtari, and Ozdaglar [FMO20], and coresets selection Borsos, Mutny, and Krause [BMK20], require \mathcal{X} to be a strict subset of \mathbb{R}^n . When dealing with such constraint sets, a common approach is to employ projection-based methods like projected gradient methods. These techniques, while widely used, entail solving nonlinear projection problems on the constraint set, which may not always be computationally feasible. The limitations of projection-based techniques has led to the development of projection-free algorithms, such as Frank Wolfe-based methods Frank and Wolfe [FW56]. Unlike projection methods, which deal with non-linear projections like ℓ_1 -norm or nuclear norm ball constraints, Frank Wolfe-based techniques involve solving linear minimization problems over \mathcal{X} , offering lower computational costs.

In the context of bilevel optimization problems, many studies have delved into constrained scenarios. However, most existing methods primarily rely on projection-based algorithms, with limited exploration of projection-free alternatives. Unfortunately, these methods often exhibit slow convergence rates or impose high computational burdens per iteration. Notably, the rapid convergence rates observed in methods like Ghadimi and Wang [GW18] are achieved by utilizing the Hessian inverse of the lower-level function, which comes at a steep price, imposing a worst-case computational cost of $\mathcal{O}(m^3)$ and limiting its applicability. To address this issue, an approximation technique for the Hessian inverse was introduced in Ghadimi and Wang [GW18] and subsequently used in studies such as [HWWY20; ABTR22]. This approximation technique introduces a vanishing bias as the number of inner steps (matrix-vector products) increases, and its computational cost scales with the condition number (κ_g) of the lower-level problem, leading to a per-iteration complexity of $\mathcal{O}(\kappa_g m^2 \log(K))$.

Contributions. To address these challenges, we introduce a novel inexact projection-free method

Table 1: Summary of results for bilevel optimization with a strongly convex lower-level function. The abbreviations ‘‘C’’, ‘‘NC’’, ‘‘PO’’, ‘‘LMO’’ stand for ‘‘convex’’, ‘‘non-convex’’, ‘‘projection oracle’’, and ‘‘linear minimization oracle’’ respectively and $\kappa_g \triangleq L_g/\mu_g$. [†] We use $poly(\kappa_g)$ as explicit dependency on κ_g is not reported. *These works primarily examined convergence rates in the stochastic setting (no deterministic result), so the results presented here are for stochastic cases.

	Reference	Oracle	Function ℓ	Assumption on	Overall Complexity	Convergence metric
			NC/C	$\nabla_y f(\mathbf{x}, \cdot)$		
Unconstrained	SUSTAIN* [KZHWWY21]	—	NC	bounded	$\tilde{\mathcal{O}}(poly(\kappa_g)m^2\epsilon^{-1.5})^\dagger$	$\mathbb{E}\ \nabla\ell(\mathbf{x}_{k^*})\ ^2$
	FSLA* [LGH22]	—	NC	bounded	$\mathcal{O}(poly(\kappa_g)m^2\epsilon^{-2})$	$\mathbb{E}\ \nabla\ell(\mathbf{x}_{k^*})\ ^2$
	AID-BiO [JYL21]	—	NC	bounded	$\mathcal{O}((\kappa_g^{3.5}m^2 + m\kappa_g^4)\epsilon^{-1})$	$\ \nabla\ell(\mathbf{x}_{k^*})\ ^2$
	F ³ SA [KKWN23]	—	NC	bounded	$\tilde{\mathcal{O}}(poly(\kappa_g)m\epsilon^{-1.5})$	$\ \nabla\ell(\mathbf{x}_{k^*})\ ^2$
	AmIGO [AM21]	—	NC	bounded	$\mathcal{O}((\kappa_g^4m^2 + m\kappa_g^4)\epsilon^{-1})$	$\ \nabla\ell(\mathbf{x}_{k^*})\ ^2$
	RAHGD [YLLJ23]	—	NC	bounded	$\mathcal{O}(\kappa_g^{3.25}m^2\epsilon^{-0.875})$	$\ \nabla\ell(\mathbf{x}_{k^*})\ ^2$
Constrained	ABA [GW18]	PO	NC	bounded	$\mathcal{O}(\kappa_g^{4.5}m^3\epsilon^{-1} + \kappa_g^5m\epsilon^{-1.25})$	$\ \nabla\ell(\mathbf{x}_{k^*})\ ^2$
			C		$\mathcal{O}(\kappa_g^{4.5}m^3\epsilon^{-0.5} + \kappa_g^5m\epsilon^{-0.75})$	$\ell(\mathbf{x}_K) - \ell(\mathbf{x}^*)$
	TTSA* [HWWY20]	PO	NC	bounded	$\tilde{\mathcal{O}}(poly(\kappa_g)m^2\epsilon^{-2.5})$	$\mathbb{E}\ \mathbf{x}_{k^*} - \text{prox}_{\rho\ell}(\mathbf{x}_{k^*})\ ^2$
			C		$\tilde{\mathcal{O}}(poly(\kappa_g)m^2\epsilon^{-4})$	$\mathbb{E}[\ell(\mathbf{x}_K) - \ell(\mathbf{x}^*)]$
	SBFW* [ABTR22]	LMO	NC	bounded	$\tilde{\mathcal{O}}(poly(\kappa_g)m^2\epsilon^{-4})$	$\mathbb{E}[\mathcal{G}(\mathbf{x}_{k^*})]$
			C		$\tilde{\mathcal{O}}(poly(\kappa_g)m^2\epsilon^{-3})$	$\mathbb{E}[\ell(\mathbf{x}_K) - \ell(\mathbf{x}^*)]$
Ours	LMO	NC	Lip. cont.	$\mathcal{O}(\kappa_g^5m^2\epsilon^{-2})$	$\mathcal{G}(\mathbf{x}_{k^*})$	
		C		$\tilde{\mathcal{O}}(\kappa_g^5m^2\epsilon^{-1})$	$\ell(\mathbf{x}_K) - \ell(\mathbf{x}^*)$	
	LMO	NC	bounded	$\mathcal{O}(\kappa_g^4m^2\epsilon^{-2})$	$\mathcal{G}(\mathbf{x}_{k^*})$	
		C		$\tilde{\mathcal{O}}(\kappa_g^4m^2\epsilon^{-1})$	$\ell(\mathbf{x}_K) - \ell(\mathbf{x}^*)$	

that attains optimal convergence rates in the studied scenarios. Remarkably, our approach demands just two matrix-vector products per iteration, resulting in a per-iteration complexity of $\mathcal{O}(m^2)$. Our main idea is to simultaneously track the trajectories of the lower-level optimal solution as well as the solution to a time-varying quadratic optimization problem. These estimators are calculated using one step of a gradient-type update and are used to estimate the hyper-gradient for a Frank Wolfe-type update. Furthermore, existing methods work under the assumption that $\nabla_y f(x, \cdot)$ is uniformly bounded which may not hold in many applications. To address this limitation, we also analyze our proposed method without the gradient boundedness assumption. Our theoretical guarantees for the proposed Inexact Bilevel Conditional Gradient (IBCG) method are as follows:

- When the hyper-objective function $\ell(x)$ is convex, and $\nabla_y f(\mathbf{x}, \cdot)$ is uniformly bounded for any $\mathbf{x} \in \mathcal{X}$, our IBCG method finds an ϵ -optimal solution after $\tilde{\mathcal{O}}(\kappa_g^4\epsilon^{-1})$ iterations. If we relax the assumption of gradient boundedness to assume Lipschitz continuity, its complexity becomes $\tilde{\mathcal{O}}(\kappa_g^5\epsilon^{-1})$.
- When $\ell(x)$ is non-convex and $\nabla_y f(\mathbf{x}, \cdot)$ is bounded, IBCG requires $\mathcal{O}(\kappa_g^4\epsilon^{-2})$ iterations to find an ϵ -stationary point. This result changes to $\mathcal{O}(\kappa_g^5\epsilon^{-2})$ when the gradient boundedness assumption is replaced by gradient Lipschitzness.

These results match the best-known complexity of projection-free algorithms for solving convex constrained single-level optimization problems [Lac16; MOJ18].

Related work. In this section, we review related work on bilevel optimization with non-asymptotic guarantees; see Table 1 for a summary of these results. As mentioned earlier, the majority of the existing works consider unconstrained bilevel problems, i.e., $\mathcal{X} = \mathbb{R}^n$. In particular, [KZHWWY21; LGH22] focused on the stochastic setting and proved an overall complexity of $\tilde{\mathcal{O}}(m^2\epsilon^{-1.5})$ and $\mathcal{O}(m^2\epsilon^{-2})$, respectively. In the deterministic setting, Yang, Ji, and Liang [YJL21] analyzed the convergence of bilevel algorithms via AID and proved a complexity of $\mathcal{O}((\kappa_g^{3.5}m^2 + m\kappa_g^4)\epsilon^{-1})$,

where κ_g denotes the condition number of the lower-level objective. By incorporating acceleration techniques, a recent work by Yang, Luo, Li, and Jordan [YLLJ23] further improved the complexity to $\mathcal{O}(\kappa_g^{3.25}m^2\epsilon^{-0.875})$. Moreover, to avoid expensive Hessian computation, Kwon, Kwon, Wright, and Nowak [KKWN23] proposed a fully first-order method with a complexity of $\tilde{\mathcal{O}}(m\epsilon^{-1.5})$.

In comparison, there are relatively few works on constrained bilevel optimization problems, which is the considered setting of this paper. Ghadimi and Wang [GW18] presented an Accelerated Bilevel Approximation (ABA) method consisting of two iterative loops. In the nonconvex setting, they demonstrated that the method achieves an overall complexity of $\mathcal{O}(\kappa_g^{4.5}m^3\epsilon^{-1})$ and $\mathcal{O}(\kappa_g^5m\epsilon^{-1.25})$ in terms of the upper-level and lower-level objective values, respectively. In convex setting, they further shaved a factor of $\mathcal{O}(\epsilon^{-0.5})$ from the complexities. However, their computational complexity is high since they must compute the Hessian inverse matrix at each iteration, incurring a per-iteration cost of $\mathcal{O}(m^3)$.

Efforts have been made to design efficient single-loop methods aimed at lowering the per-iteration expenses. Notably, similar to our proposed IBCG method, approaches in [DAVM22; LGH22] demand only two matrix-vector products per iteration. However, these works have exclusively addressed unconstrained bilevel problems. Built upon the work of Ghadimi and Wang [GW18], a Two-Timescale Stochastic Approximation (TTSA) algorithm has been proposed by Hong, Wai, Wang, and Yang [HWY20] for constrained bilevel problems in the stochastic setting, which is shown to achieve a complexity of $\tilde{\mathcal{O}}(m^2\epsilon^{-2.5})$ and $\tilde{\mathcal{O}}(m^2\epsilon^{-4})$ in nonconvex and convex settings, respectively. Concurrently, Shen and Chen [SC23] introduced a penalty-based bilevel gradient descent (PBGD) algorithm, categorizing it as a projection-based method. In their work, they focused on scenarios where the lower-level function satisfies the Polyak-Lojasiewicz condition.

It should be noted that the above methods require a projection onto the set \mathcal{X} at every iteration. In contrast, our proposed method is projection-free and only requires access to a linear solver, which is suitable for settings where projection is computationally costly; e.g., when \mathcal{X} is a nuclear-norm ball. A closely related study is the work by Akhtar, Bedi, Thomdapu, and Rajawat [ABTR22], where they presented a projection-free algorithm named SBFW for *stochastic* bilevel optimization problems. Their findings demonstrate that their method attains a complexity of $\mathcal{O}(m^2\epsilon^{-4})$ for nonconvex scenarios and $\mathcal{O}(m^2\epsilon^{-3})$ for convex settings, respectively.

Lastly, concurrent papers like [LMYZZ20; SJGL22; CXZ23] explored scenarios where the lower-level problem can possess multiple minima. Given the increased complexity of this generalized setting, their theoretical results are comparatively weaker, offering either asymptotic guarantees or slower convergence rates.

2 Preliminaries

2.1 Motivating Examples

The bilevel optimization formulation in (1) finds applications in various ML problems, including matrix completion Yokota and Hontani [YH17], meta-learning Rajeswaran, Finn, Kakade, and Levine [RFKL19], data hyper-cleaning Shaban, Cheng, Hatch, and Boots [SCHB19], hyper-parameter optimization Franceschi, Frasconi, Salzo, Grazzi, and Pontil [FFSGP18b], and more. Next, we delve into two specific examples.

Matrix Completion with Denoising: Consider the matrix completion problem, where the

objective is to recover missing items from noisy observations of a subset of the matrix’s entries. Typically, in noiseless scenarios, the data matrix can be represented as a low-rank matrix, justifying the use of the nuclear norm constraint. However, in applications such as image processing and collaborative filtering, noisy observations are common, and relying solely on the nuclear norm constraint can lead to suboptimal results [MD21; YH17]. To address this issue, one approach to incorporate denoising into the matrix completion problem is by formulating it as a bilevel optimization problem Akhtar, Bedi, Thomdapu, and Rajawat [ABTR22], expressed as:

$$\begin{aligned} & \min_{\|\mathbf{X}\|_* \leq \alpha} \frac{1}{|\Omega_1|} \sum_{(i,j) \in \Omega_1} (\mathbf{X}_{i,j} - \mathbf{Y}_{i,j})^2 \\ \text{s.t. } & \mathbf{Y} \in \underset{\mathbf{V}}{\operatorname{argmin}} \left\{ \frac{1}{|\Omega_2|} \sum_{(i,j) \in \Omega_2} (\mathbf{V}_{i,j} - \mathbf{M}_{i,j})^2 + \lambda_1 \mathcal{R}(\mathbf{V}) + \lambda_2 \|\mathbf{X} - \mathbf{V}\|_F^2 \right\}, \end{aligned} \quad (2)$$

where $\mathbf{M} \in \mathbb{R}^{n \times m}$ is the given incomplete noisy matrix. Moreover, $\Omega_1 \subseteq \Omega$ and $\Omega_2 \subseteq \Omega$ where Ω is the set of observable entries, and $\mathcal{R}(\mathbf{V})$ is a regularization term to induce sparsity, e.g., ℓ_1 -norm or pseudo-Huber loss, λ_1 and λ_2 are regularization parameters. The presence of the nuclear norm constraint poses a significant challenge in (2). This constraint renders the problem computationally demanding, often making projection-based algorithms impractical. Consequently, there is a compelling need to develop and employ projection-free methods to overcome these computational limitations.

Multi-Task Learning: Multi-Task Learning (MTL) is a machine learning paradigm that leverages insights from multiple related tasks to enhance overall performance and generalization. In essence, when faced with T learning tasks, whether all or a subset are related, MTL seeks to jointly learn these tasks. This joint learning process aims to improve each task’s model by tapping into the knowledge contained within all or some of the tasks. In the supervised setting, research has explored various approaches, including the Multi-task Feature Learning (MTFL) method Zhang and Yeung [ZY14]. In MTFL, the goal is to minimize the overall loss function while learning the feature covariance matrix $\Omega \in \mathbb{R}^{T \times T}$ for all the tasks. Considering a model parameter $W = [w_1, \dots, w_T] \in \mathbb{R}^{d \times T}$ where $w_i \in \mathbb{R}^d$ denotes the model parameter for task i , Zhang and Yeung [ZY14] formulated this problem as $\min_{W, \Omega} \{ \sum_{i=1}^T L_i(w_i) + \lambda \operatorname{Tr}(W \Omega^{-1} W) \mid \Omega \succeq 0, \operatorname{Tr}(\Omega) \leq c \}$ for some $c > 0$ where $L_i(\cdot; \mathcal{D}_i)$ denotes the loss function of task i given dataset \mathcal{D}_i and $\operatorname{Tr}(\cdot)$ denotes the trace of a square matrix. This problem can also be written as a bilevel optimization problem. To do so, consider \mathcal{D}_i^{tr} and \mathcal{D}_i^{val} as training and validation datasets for task i , respectively. In this problem, the upper-level problem seeks to identify the best covariance matrix by minimizing the loss function over the validation dataset, while the lower-level problem aims to find the best model for the training set given a covariance matrix Ω . Specifically, for $\lambda_1, \lambda_2 > 0$, the MTLF problem can be written as

$$\begin{aligned} & \min_{\substack{\Omega \succeq 0 \\ \operatorname{Tr}(\Omega) \leq c}} \sum_{i=1}^T L_i(w_i^*(\Omega); \mathcal{D}_i^{val}) \\ \text{s.t. } & W^*(\Omega) \in \underset{W}{\operatorname{argmin}} \left\{ \sum_{i=1}^T L_i(w_i; \mathcal{D}_i^{tr}) + \lambda_1 \|W\|_F^2 + \lambda_2 \operatorname{Tr}(W \Omega^{-1} W^T) \right\}, \end{aligned} \quad (3)$$

which is an instance of the constrained bilevel problem (1).

2.2 Assumptions and Definitions

In this subsection, we discuss the definitions and assumptions required throughout the paper. We begin by discussing the assumptions on the upper-level and lower-level objective functions, respectively.

Assumption 2.1. $\nabla_x f(\mathbf{x}, \mathbf{y})$ and $\nabla_y f(\mathbf{x}, \mathbf{y})$ are Lipschitz continuous w.r.t $(\mathbf{x}, \mathbf{y}) \in \mathcal{X} \times \mathbb{R}^m$ such that for any $\mathbf{x}, \bar{\mathbf{x}} \in \mathcal{X}$ and $\mathbf{y}, \bar{\mathbf{y}} \in \mathbb{R}^m$ we have:

$$(i) \|\nabla_x f(\mathbf{x}, \mathbf{y}) - \nabla_x f(\bar{\mathbf{x}}, \bar{\mathbf{y}})\| \leq L_{xx}^f \|\mathbf{x} - \bar{\mathbf{x}}\| + L_{xy}^f \|\bar{\mathbf{y}} - \mathbf{y}\|,$$

$$(ii) \|\nabla_y f(\mathbf{x}, \mathbf{y}) - \nabla_y f(\bar{\mathbf{x}}, \bar{\mathbf{y}})\| \leq L_{yx}^f \|\mathbf{x} - \bar{\mathbf{x}}\| + L_{yy}^f \|\mathbf{y} - \bar{\mathbf{y}}\|.$$

Assumption 2.2. $g(\mathbf{x}, \mathbf{y})$ satisfies the following conditions:

(i) $\forall \mathbf{x} \in \mathcal{X}$, $g(\mathbf{x}, \cdot)$ is twice continuously differentiable. Moreover, $\nabla_y g(\cdot, \cdot)$ is continuously differentiable.

(ii) $\forall \mathbf{x} \in \mathcal{X}$, $\nabla_y g(\mathbf{x}, \cdot)$ is Lipschitz continuous with constant $L_g \geq 0$. Moreover, $\forall \mathbf{y} \in \mathbb{R}^m$, $\nabla_y g(\cdot, \mathbf{y})$ is Lipschitz continuous with constant $C_{yx}^g \geq 0$.

(iii) $\forall \mathbf{x} \in \mathcal{X}$, $g(\mathbf{x}, \cdot)$ is μ_g -strongly convex.

(iv) $\forall \mathbf{x} \in \mathcal{X}$, $\nabla_{yx}^2 g(\mathbf{x}, \mathbf{y}) \in \mathbb{R}^{n \times m}$ and $\nabla_{yy}^2 g(\mathbf{x}, \mathbf{y})$ are Lipschitz continuous with respect to $(\mathbf{x}, \mathbf{y}) \in \mathcal{X} \times \mathbb{R}^m$, and with constant $L_{yx}^g \geq 0$ and $L_{yy}^g \geq 0$, respectively.

Remark 2.1. Considering Assumption 2.2-(ii), we can conclude that $\|\nabla_{yx}^2 g(\mathbf{x}, \mathbf{y})\|$ is bounded above by constant $C_{yx}^g \geq 0$ for any $(\mathbf{x}, \mathbf{y}) \in \mathcal{X} \times \mathbb{R}^m$.

Next, we present essential properties of the bilevel problem in (1) based on the aforementioned assumptions. Firstly, through standard analysis under Assumption 2.2, it is evident that the optimal solution trajectory of the lower-level problem denoted as $\mathbf{y}^*(\mathbf{x})$, is Lipschitz continuous, as previously discussed in [GW18].

Secondly, when aiming to develop a method with a guaranteed convergence, one key requirement is demonstrating the Lipschitz continuity of the gradient of the single-level objective function. In bilevel optimization literature, this often necessitates assuming the boundedness of $\nabla_y f(\mathbf{x}, \mathbf{y})$ for any $\mathbf{x} \in \mathcal{X}$ and $\mathbf{y} \in \mathbb{R}^m$, as seen in [GW18; YJL21; HWWY20; ABTR22]. However, in contrast, our paper establishes that this condition is solely required for the gradient map $\nabla_y f(\mathbf{x}, \mathbf{y})$ when restricted to the optimal trajectory of the lower-level problem. Specifically, we demonstrate that it suffices to prove the boundedness of $\nabla_y f(\mathbf{x}, \mathbf{y}^*(\mathbf{x}))$ for any $\mathbf{x} \in \mathcal{X}$, a result derivable from the boundedness of constraint set \mathcal{X} .

Lastly, employing the above findings, we can assert that the gradient of the single-level objective function denoted as $\nabla \ell(\mathbf{x})$, is also Lipschitz continuous. This outcome constitutes a fundamental element in the subsequent convergence analysis of our proposed method in the following section. The detailed formal statements of these results are presented in the subsequent lemma.

Lemma 2.1. Suppose Assumptions 2.1 and 2.2 hold. Then for any $\mathbf{x}, \bar{\mathbf{x}} \in \mathcal{X}$, the following results hold.

$$(I) \|\mathbf{y}^*(\mathbf{x}) - \mathbf{y}^*(\bar{\mathbf{x}})\| \leq \mathbf{L}_y \|\mathbf{x} - \bar{\mathbf{x}}\|, \text{ where } \mathbf{L}_y \triangleq \frac{C_{yx}^g}{\mu_g}.$$

$$(II) \|\nabla_y f(\mathbf{x}, \mathbf{y}^*(\mathbf{x}))\| \leq C_y^f, \text{ where } C_y^f \triangleq \left(L_{yx}^f + \frac{L_{yy}^f C_{yx}^g}{\mu_g} \right) D_{\mathcal{X}} + \|\nabla_y f(\mathbf{x}^*, \mathbf{y}^*(\mathbf{x}^*))\|.$$

$$(III) \|\nabla \ell(\mathbf{x}) - \nabla \ell(\bar{\mathbf{x}})\| \leq \mathbf{L}_\ell \|\mathbf{x} - \bar{\mathbf{x}}\|, \text{ where } \mathbf{L}_\ell \triangleq L_{xx}^f + L_{xy}^f \mathbf{L}_y + C_{yx}^g \mathbf{C}_v + \frac{C_y^f}{\mu_g} L_{yx}^g (1 + \mathbf{L}_y).$$

To measure the quality of the solution at each iteration in the nonconvex setting, we use the standard Frank-Wolfe gap function associated with the hyper-function defined below.

Definition 2.1. *The Frank-Wolfe gap of ℓ over the set \mathcal{X} is*

$$\mathcal{G}(\mathbf{x}) \triangleq \max_{\mathbf{s} \in \mathcal{X}} \{\langle \nabla \ell(\mathbf{x}), \mathbf{x} - \mathbf{s} \rangle\}. \quad (4)$$

When the hyper-function ℓ is non-convex, we use its Frank-Wolfe gap as our criteria for convergence which is a standard performance metric for constrained non-convex settings; see, e.g., [ZSMHK20; RSPS16]. In the convex setting, we simply use the suboptimality gap function, i.e., $\ell(\mathbf{x}) - \ell(\mathbf{x}^*)$, for capturing the suboptimality of the solution.

3 Proposed Method

As previously discussed in Section 1, the bilevel problem presented in (1) can be conceptualized as a single-level minimization problem $\min_{\mathbf{x} \in \mathcal{X}} \ell(\mathbf{x})$. Given Assumptions 2.1 and 2.2, it can be shown that the gradient of the hyper-objective $\ell(\cdot)$ can be expressed as follows:

$$\nabla \ell(\mathbf{x}) = \nabla_x f(\mathbf{x}, \mathbf{y}^*(\mathbf{x})) + \mathbf{J}\mathbf{y}^*(\mathbf{x}) \nabla_y f(\mathbf{x}, \mathbf{y}^*(\mathbf{x})), \quad (5)$$

where $\mathbf{J}\mathbf{y}^*(\mathbf{x}) = -\nabla_{yx}^2 g(\mathbf{x}, \mathbf{y}^*(\mathbf{x})) [\nabla_{yy}^2 g(\mathbf{x}, \mathbf{y}^*(\mathbf{x}))]^{-1}$; see [GW18]. Implementing first-order methods for solving the single-level minimization problem poses a significant challenge due to the costly operation of matrix inversion and the requirement of finding the exact optimal solution for the lower-level problem. We further elaborate on these issues in the upcoming section and will discuss how our proposed method overcomes them.

3.1 Main Algorithm

As discussed above, there are major limitations in a naive implementation of a first-order method for solving (1). To propose a practical conditional gradient-based method, we revisit the problem's structure. In particular, the gradient of the single-level problem in (5) can be rewritten as follows

$$\nabla \ell(\mathbf{x}) = \nabla_x f(\mathbf{x}, \mathbf{y}^*(\mathbf{x})) - \nabla_{yx}^2 g(\mathbf{x}, \mathbf{y}^*(\mathbf{x})) \mathbf{v}(\mathbf{x}), \quad (6a)$$

$$\text{where } \mathbf{v}(\mathbf{x}) \triangleq [\nabla_{yy}^2 g(\mathbf{x}, \mathbf{y}^*(\mathbf{x}))]^{-1} \nabla_y f(\mathbf{x}, \mathbf{y}^*(\mathbf{x})). \quad (6b)$$

In this formulation, the effect of Hessian inversion is presented in a separate term $\mathbf{v}(\mathbf{x})$ which can be viewed as the solution of the following *parametric* quadratic problem

$$\begin{aligned} \mathbf{v}(\mathbf{x}) = & \quad (7) \\ \operatorname{argmin}_{\mathbf{v}} & \frac{1}{2} \mathbf{v}^\top \nabla_{yy}^2 g(\mathbf{x}, \mathbf{y}^*(\mathbf{x})) \mathbf{v} - \nabla_y f(\mathbf{x}, \mathbf{y}^*(\mathbf{x}))^\top \mathbf{v}. \end{aligned}$$

Our main idea is to provide *nested* approximations for the true gradient in (5) by estimating trajectories of $\mathbf{y}^*(\mathbf{x})$ and $\mathbf{v}(\mathbf{x})$. To ensure convergence, we carefully control the algorithm's progress in terms of variable \mathbf{x} and limit the error introduced by these approximations. More specifically, at each iteration $k \geq 0$, given an iterate \mathbf{x}_k and an approximated solution of the lower-level problem

Algorithm 1 Inexact Bilevel Conditional Gradient (IBCG) Method

- 1: **Input:** $\{\gamma_k, \eta_k\}_k \subseteq \mathbb{R}_+, \alpha > 0, \mathbf{x}_0 \in \mathcal{X}, \mathbf{y}_0 \in \mathbb{R}^m$
 - 2: **Initialization:** $\mathbf{w}^0 \leftarrow \mathbf{y}^0$
 - 3: **for** $k = 0, \dots, K - 1$ **do**
 - 4: $\mathbf{w}_{k+1} \leftarrow (I - \eta_k \nabla_{yy}^2 g(\mathbf{x}_k, \mathbf{y}_k)) \mathbf{w}_k + \eta_k \nabla_y f(\mathbf{x}_k, \mathbf{y}_k)$
 - 5: $F_k \leftarrow \nabla_x f(\mathbf{x}_k, \mathbf{y}_k) - \nabla_{yx}^2 g(\mathbf{x}_k, \mathbf{y}_k) \mathbf{w}_{k+1}$
 - 6: Compute $\mathbf{s}_k \leftarrow \operatorname{argmin}_{\mathbf{s} \in \mathcal{X}} \langle F_k, \mathbf{s} \rangle$
 - 7: $\mathbf{x}_{k+1} \leftarrow (1 - \gamma_k) \mathbf{x}_k + \gamma_k \mathbf{s}_k$
 - 8: $\mathbf{y}_{k+1} \leftarrow \mathbf{y}_k - \alpha \nabla_y g(\mathbf{x}_{k+1}, \mathbf{y}_k)$
 - 9: **end for**
-

\mathbf{y}_k we first consider an approximated solution $\tilde{\mathbf{v}}(\mathbf{x}_k)$ of (7) by replacing $\mathbf{y}^*(\mathbf{x}_k)$ with its currently available approximation, i.e., \mathbf{y}_k , which leads to the following quadratic programming

$$\tilde{\mathbf{v}}(\mathbf{x}_k) \triangleq \operatorname{argmin}_{\mathbf{v}} \frac{1}{2} \mathbf{v}^\top \nabla_{yy}^2 g(\mathbf{x}_k, \mathbf{y}_k) \mathbf{v} - \nabla_y f(\mathbf{x}_k, \mathbf{y}_k)^\top \mathbf{v}.$$

Then $\tilde{\mathbf{v}}(\mathbf{x}_k)$ is approximated with an iterate \mathbf{w}_{k+1} obtained by taking one step of gradient descent with respect to the above objective function as follows,

$$\mathbf{w}_{k+1} \leftarrow \mathbf{w}_k - \eta_k (\nabla_{yy}^2 g(\mathbf{x}_k, \mathbf{y}_k) \mathbf{w}_k - \nabla_y f(\mathbf{x}_k, \mathbf{y}_k)),$$

for some step-size $\eta_k \geq 0$. This generates an increasingly accurate sequence $\{\mathbf{w}_k\}_{k \geq 0}$ that tracks the sequence $\{\mathbf{v}(\mathbf{x}_k)\}_{k \geq 0}$. Next, given approximated solutions \mathbf{y}_k and \mathbf{w}_{k+1} for $\mathbf{y}^*(\mathbf{x}_k)$ and $\mathbf{v}(\mathbf{x}_k)$, respectively, we can construct a direction to estimate the hyper-gradient $\nabla \ell(\mathbf{x}_k)$ in (6a). To this end, we construct a direction $F_k = \nabla_x f(\mathbf{x}_k, \mathbf{y}_k) - \nabla_{yx}^2 g(\mathbf{x}_k, \mathbf{y}_k) \mathbf{w}_{k+1}$, which determines the next iteration \mathbf{x}_{k+1} using a Frank-Wolfe type update, i.e.,

$$\mathbf{s}_k \leftarrow \operatorname{argmin}_{\mathbf{s} \in \mathcal{X}} \langle F_k, \mathbf{s} \rangle, \quad \mathbf{x}_{k+1} \leftarrow (1 - \gamma_k) \mathbf{x}_k + \gamma_k \mathbf{s}_k.$$

for some step-size $\gamma_k \in [0, 1]$. Finally, having an updated decision variable \mathbf{x}_{k+1} we estimate the lower-level optimal solution $\mathbf{y}^*(\mathbf{x}_{k+1})$ by performing another gradient descent step with respect to the lower-level function $g(\mathbf{x}_k, \mathbf{y}_k)$ with step-size $\alpha > 0$ to generate a new iterate \mathbf{y}_{k+1} as follows:

$$\mathbf{y}_{k+1} \leftarrow \mathbf{y}_k - \alpha \nabla_y g(\mathbf{x}_{k+1}, \mathbf{y}_k).$$

Our proposed inexact bilevel conditional gradient (IBCG) method is summarized in Algorithm 1.

4 Convergence Analysis

To establish the convergence guarantee of the proposed IBCG method, we first present the following lemma that quantifies the error between the approximated direction F_k and the exact hyper-gradient $\nabla \ell(\mathbf{x}_k)$. This involves providing upper bounds on the errors induced by our nested approximation technique discussed above, i.e., $\|\mathbf{w}_{k+1} - \mathbf{v}(\mathbf{x}_k)\|$ and $\|\mathbf{y}_{k+1} - \mathbf{y}^*(\mathbf{x}_{k+1})\|$, as well as Lemma 2.1.

Lemma 4.1. *Suppose Assumptions 2.1-2.2 hold and let $\beta \triangleq (L_g - \mu_g)/(L_g + \mu_g)$ and $\mathbf{C}_v \triangleq \frac{L_{yx}^f + L_{yy}^f \mathbf{L}_y}{\mu_g} + \frac{C_y^f L_{yy}^g}{\mu_g^2} (1 + \mathbf{L}_y)$. Moreover, let $\{\mathbf{x}_k, \mathbf{y}_k, \mathbf{w}_k\}_{k \geq 0}$ be the sequence generated by Algorithm*

1 with step-sizes $\gamma_k = \gamma \in (0, 1]$, $\eta_k = \eta < \frac{1-\beta}{\mu_g}$, and $\alpha = 2/(\mu_g + L_g)$. Then, for any $k \geq 0$

$$\begin{aligned} \|\nabla \ell(\mathbf{x}_k) - F_k\| &\leq \mathbf{C}_2(\beta^k D_0^y + \frac{\gamma\beta \mathbf{L}_y}{1-\beta} D_{\mathcal{X}}) + C_{yx}^g(\rho^{k+1} \|\mathbf{w}_0 - \mathbf{v}(\mathbf{x}_0)\| + \frac{\gamma\rho \mathbf{C}_v}{1-\rho} D_{\mathcal{X}} \\ &\quad + \frac{\eta \mathbf{C}_1}{\rho - \beta} \rho^{k+2} D_0^y + \frac{\gamma\beta \mathbf{C}_1 \mathbf{L}_y}{(1-\rho)(1-\beta)} D_{\mathcal{X}}), \end{aligned} \quad (8)$$

where $\rho \triangleq 1 - \eta\mu_g$, $\mathbf{C}_1 \triangleq L_{yy}^g \frac{C_y^f}{\mu_g} + L_{yy}^f$, $\mathbf{C}_2 \triangleq L_{xy}^f + L_{yx}^g \frac{C_y^f}{\mu_g}$, and $D_0^y \triangleq \|\mathbf{y}_0 - \mathbf{y}^*(\mathbf{x}_0)\|$.

Lemma 4.1 provides an upper bound on the error of the approximated gradient direction F_k . This bound encompasses two types of terms: those that decrease exponentially fast and others that are influenced by the parameter γ . The selection of the appropriate value for γ is crucial because if it is too large, it can introduce significant errors in the algorithm's direction, and if it is too small, it can impede progress in the iterations. Therefore, it is essential to choose an appropriate γ based on the algorithm's overall progress. By utilizing the insights from Lemma 4.1, we can set a limit on the gap function and ensure a guaranteed rate of convergence through the appropriate choice of γ .

Next, we present our convergence guarantees for the IBCG method. We start by considering the scenario where the hyper-objective function $\ell(\cdot)$ exhibits convexity. Before presenting our results, we highlight two generic examples that yield a convex hyper-objective function ℓ : (i) When f is jointly convex, and $y^*(\cdot)$ is an affine map. (ii) In cases where we encounter a min-max optimization problem of the form $\min_{\mathbf{x} \in \mathcal{X}} \max_{\mathbf{y} \in \mathbb{R}^m} f(\mathbf{x}, \mathbf{y})$, and f demonstrates convexity in \mathbf{x} and strong concavity in \mathbf{y} . This problem can be reformulated into a bilevel optimization problem by defining $g(\mathbf{x}, \mathbf{y}) = -f(\mathbf{x}, \mathbf{y})$, which results in a convex hyper-objective function $\ell(\mathbf{x}) = \max_{\mathbf{y}} f(\mathbf{x}, \mathbf{y})$.

Theorem 4.2 (Convex bilevel). *Suppose Assumptions 2.1 and 2.2 hold. Let $\{\mathbf{x}_k\}_{k=0}^{K-1}$ be the sequence generated by Algorithm 1 with step-sizes specified as in Lemma 4.1. If $\ell(\mathbf{x})$ is convex, then for all $K \geq 1$,*

$$\ell(\mathbf{x}_K) - \ell(\mathbf{x}^*) \leq (1 - \gamma)^K (\ell(\mathbf{x}_0) - \ell(\mathbf{x}^*)) + \sum_{k=0}^{K-1} (1 - \gamma)^{K-k} \mathcal{R}_k(\gamma), \quad (9)$$

where $\mathcal{R}_k(\gamma) \triangleq \gamma \mathbf{C}_2 \beta^k D_0^y D_{\mathcal{X}} + \frac{\gamma^2 \mathbf{C}_2 D_{\mathcal{X}}^2 \mathbf{L}_y \beta}{1-\beta} + C_{yx}^g [\gamma D_{\mathcal{X}} \rho^{k+1} \|\mathbf{w}_0 - \mathbf{v}(\mathbf{x}_0)\| + \frac{\gamma^2 D_{\mathcal{X}}^2 \rho \mathbf{C}_v}{1-\rho} + \frac{\gamma D_{\mathcal{X}} D_0^y \mathbf{C}_1 \eta \rho^{k+2}}{\rho - \beta} + \frac{\gamma^2 D_{\mathcal{X}}^2 \mathbf{L}_y \mathbf{C}_1 \beta \eta}{(1-\beta)(1-\rho)}] + \frac{1}{2} \mathbf{L}_\ell \gamma^2 D_{\mathcal{X}}^2$.

Theorem 4.2 establishes that in the convex setting, the suboptimality of the function ℓ is bounded above by an upper bound composed of two components. The first component exhibits a linear convergence rate and decreases exponentially, while the second component stems from errors in nested approximations and can be alleviated by reducing the step-size γ . Therefore, by properly choosing the step-size γ , we can attain a guaranteed convergence rate, as outlined in the following Corollary.

Corollary 4.3. *Let $\{\mathbf{x}_k\}_{k=0}^{K-1}$ be the sequence generated by Algorithm 1 with step-size $\gamma_k = \gamma = \frac{\log(K)}{K}$. Under the premises of Theorem 4.2 we have that $\ell(\mathbf{x}_K) - \ell(\mathbf{x}^*) \leq \epsilon$ after $\mathcal{O}(\kappa_g^5 \epsilon^{-1} \log(\epsilon^{-1}))$ iterations. Furthermore, assuming that $\nabla_y f(\mathbf{x}, \cdot)$ is uniformly bounded for any $\mathbf{x} \in \mathcal{X}$, we have that $\ell(\mathbf{x}_k) - \ell(\mathbf{x}^*) \leq \epsilon$ after $\mathcal{O}(\kappa_g^4 \epsilon^{-1} \log(\epsilon^{-1}))$ iterations.*

By leveraging the result of Theorem 4.2, the above Corollary characterizes the complexity of IBCG in the convex setting. Specifically, when we set $\gamma = \log(K)/K$, the total iteration complexity of

IBCG to find an ϵ -optimal solution is $\mathcal{O}(\kappa_g^5 \epsilon^{-1} \log(\epsilon^{-1}))$, where κ_g represents the condition number of the lower-level problem. Additionally, if the gradient of the upper-level is bounded, the required complexity is further reduced to $\mathcal{O}(\kappa_g^4 \epsilon^{-1} \log(\epsilon^{-1}))$. Now we turn to the case where $\ell(\cdot)$ is nonconvex.

Theorem 4.4 (Non-convex bilevel). *Suppose Assumptions 2.1 and 2.2 hold. Let $\{\mathbf{x}_k\}_{k=0}^{K-1}$ be the iterates generated by Algorithm 1 with step-sizes specified as in Lemma 4.1. Then,*

$$\begin{aligned} \mathcal{G}_{k^*} \leq & \frac{\ell(\mathbf{x}_0) - \ell(\mathbf{x}^*)}{K\gamma} + \frac{\gamma \mathbf{C}_2 D_{\mathcal{X}} \mathbf{L}_y \beta}{1 - \beta} + \frac{\gamma D_{\mathcal{X}}^2 \rho \mathbf{C}_v C_{yx}^g \rho}{1 - \rho} + \frac{\gamma D_{\mathcal{X}}^2 C_{yx}^g \mathbf{L}_y \mathbf{C}_1 \beta \eta}{(1 - \beta)(1 - \rho)} + \frac{1}{2} \mathbf{L}_\ell \gamma D_{\mathcal{X}}^2 + \frac{\mathbf{C}_2 D_0^y D_{\mathcal{X}} \beta}{K(1 - \beta)} \\ & + \frac{D_{\mathcal{X}} C_{yx}^g \rho \|\mathbf{w}_0 - \mathbf{v}(\mathbf{x}_0)\|}{K(1 - \rho)} + \frac{D_{\mathcal{X}} D_0^y C_{yx}^g \mathbf{C}_1 \eta \rho^2}{K(\rho - \beta)(1 - \rho)}, \end{aligned}$$

where \mathcal{G}_{k^*} is defined as $\mathcal{G}_{k^*} \triangleq \min_{0 \leq k \leq K-1} \mathcal{G}(\mathbf{x}_k)$.

Theorem 4.4 establishes an upper bound on the Frank-Wolfe gap for the iterates generated by IBCG. It shows that the Frank-Wolfe gap vanishes when the step-size γ is properly selected. Specifically, setting $\gamma = \mathcal{O}(1/\sqrt{K})$ as outlined in the next corollary leads to a convergence rate of $\mathcal{O}(1/\sqrt{K})$.

Corollary 4.5. *Let $\{\mathbf{x}_k\}_{k=0}^{K-1}$ be the sequence generated by Algorithm 1 with step-size $\gamma_k = \gamma = \kappa_g^{-2.5} K^{-0.5}$, then there exists $k^* \in \{0, 1, \dots, K-1\}$ such that $\mathcal{G}_{k^*} \leq \epsilon$ after $\mathcal{O}(\kappa_g^5 \epsilon^{-2})$ iterations. Furthermore, if $\nabla_y f(\mathbf{x}, \cdot)$ is uniformly bounded for any $\mathbf{x} \in \mathcal{X}$, selecting $\gamma_k = \gamma = \kappa_g^{-2} K^{-0.5}$ implies that $\mathcal{G}_{k^*} \leq \epsilon$ after $\mathcal{O}(\kappa_g^4 \epsilon^{-2})$ iterations.*

Remark 4.1. Our proposed method's efficiency stands out due to its requirement of just two matrix-vector multiplications. Furthermore, our results establish the state-of-the-art bounds for the considered setting. In the convex setting, our complexity result is near-optimal among projection-free methods for single-level optimization problems, as it is known that the worst-case complexity of such methods is $\mathcal{O}(1/\epsilon)$ [Jag13; Lan13]. In the nonconvex setting, our complexity result matches the best-known bound of $\mathcal{O}(1/\epsilon^2)$ within the family of projection-free methods for single-level optimization problems [Jag13; Lan13]. This underscores the efficiency and effectiveness of our approach in this specific context.

Remark 4.2. One of the key distinctions between our IBCG method and SBFW lies in how we approximate the Hessian matrix inversion within the hyper-gradient equation in (5). In our approach, we compute $\tilde{\mathbf{v}}(\mathbf{x}_k)$ by computing a single step of gradient descent on the quadratic function presented in (7). This leads to a single-loop algorithm that demands only two matrix-vector products per iteration. Considering the general scenario where $\nabla_y f(\mathbf{x}, \cdot)$ may not be bounded, the error of approximating $\mathbf{v}(\mathbf{x}_k)$ can be bounded as $\|\mathbf{w}_k - \mathbf{v}(\mathbf{x}_k)\| \leq \mathcal{O}((\frac{\kappa_g - 1}{\kappa_g + 1})^k + \kappa_g^{2.5}/\sqrt{k})$ by selecting γ as in Corollary 4.5 – see Lemma B.3 in Appendix for details. In contrast, SBFW constructs a biased stochastic estimate of the Hessian inverse matrix, namely \mathbf{H}_k , such that $\|\mathbf{H}_k \nabla_y f(\mathbf{x}_k, \mathbf{y}_k) - \mathbf{v}(\mathbf{x}_k)\| \leq \mathcal{O}(\kappa_g^2/\sqrt{k})$ at the cost of computing $\mathcal{O}(\kappa_g \log(k))$ matrix-vector products per iteration. Consequently, our analysis is fundamentally different from those in prior work and presents a novel contribution within the realm of projection-free algorithms.

5 Numerical Experiments

In this section, we test our method for solving different bilevel optimization problems and compare it with methods proposed in [HWWY20; ABTR22]. All the experiments are performed with Intel(R) Core(TM) i5-10210U CPU @ 1.60GHz. Additional numerical experiments are presented in Appendix G.

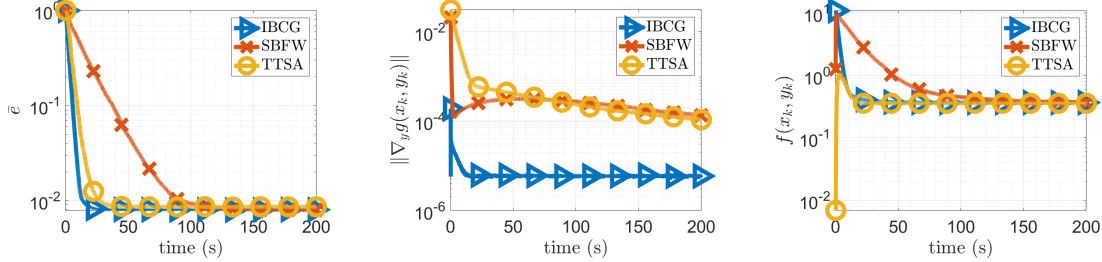


Figure 1: Performance of IBCG vs SBFW and TTSA on problem (2) for synthetic dataset. Plots from left to right: normalized error (\bar{e}), $\|\nabla_y g(\mathbf{x}_k, \mathbf{y}_k)\|$, and $f(\mathbf{x}_k, \mathbf{y}_k)$ over time.

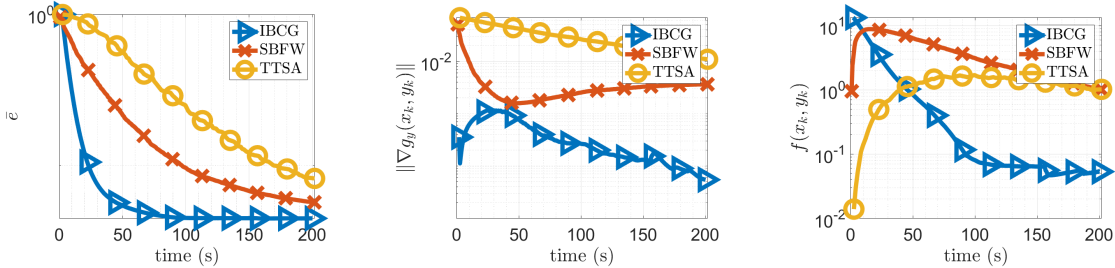


Figure 2: Performance of IBCG (blue) vs SBFW (red) and TTSA (yellow) on problem (2) for the MovieLens dataset. Plots from left to right: normalized error (\bar{e}), $\|\nabla_y g(\mathbf{x}_k, \mathbf{y}_k)\|$, and $f(\mathbf{x}_k, \mathbf{y}_k)$ over time.

5.1 Matrix Completion with Denoising

In this section, we evaluate the performance of our IBCG algorithm in solving the matrix completion with denoising problem outlined in (2). We conduct experiments using both synthetic and real datasets to assess its effectiveness.

Synthetic dataset. The experimental setup we adopt is aligned with the methodology used in Mokhtari, Hassani, and Karbasi [MHK20]. In particular, we create an observation matrix $M = \hat{X} + E$. In this setting $\hat{X} = WW^T$ where $W \in \mathbb{R}^{n \times r}$ containing normally distributed independent entries, and $E = \hat{n}(L + L^T)$ is a noise matrix where $L \in \mathbb{R}^{n \times n}$ containing normally distributed independent entries and $\hat{n} \in (0, 1)$ is the noise factor. During the simulation process, we set $n = 250$, $r = 10$, and $\alpha = \|\hat{X}\|_*$. Additionally, we establish the set of observed entries Ω by randomly sampling entries of M with a probability of 0.8. Initially, we set $\hat{n} = 0.5$ and employ the IBCG algorithm to solve the problem described in (2). We compare our method with TTSA Hong, Wai, Wang, and Yang [HWWY20] and SBFW Akhtar, Bedi, Thomdapu, and Rajawat [ABTR22]. We set $\lambda_1 = \lambda_2 = 0.05$, and set the maximum number of iteration as 10^4 . It should be noted that we consider pseudo-Huber loss defined by $\mathcal{R}_\delta(\mathbf{V}) = \sum_{i,j} \delta^2(\sqrt{1 + (\mathbf{V}_{ij}/\delta)^2} - 1)$ as a regularization term to induce sparsity and set $\delta = 0.9$. The performance is analyzed based on the normalized error, defined as $\bar{e} := \sum_{(i,j) \in \Omega} (X_{i,j} - \hat{X}_{i,j})^2 / \sum_{(i,j) \in \Omega} \hat{X}_{i,j}^2$, where X is the matrix generated by the algorithm. Note that, despite being a projection-free method, the SBFW algorithm exhibits a slower theoretical convergence rate. In comparison, our proposed method surpasses TTSA by attaining lower values of $\|\nabla_y g(\mathbf{x}_k, \mathbf{y}_k)\|$ and demonstrating slightly better performance in terms of the normalized error values, as shown in Fig. 1. This gain is due to the projection-free nature of our method, allowing for fast convergence without the need for complex projections at each iteration.

Real dataset. To assess IBCG’s scalability, we conducted experiments using the MovieLens datasets, containing large matrices of user-generated movie ratings (ranging from 1 to 5). We

employed the MovieLens 100k dataset, encompassing 10^5 ratings from 1000 individuals and 1700 movies. This dataset is represented by the observation matrix $M \in \mathbb{R}^{1000 \times 1700}$. Fig. 2 illustrates the performance of considered methods. Our proposed method exhibits faster convergence in terms of normalized error (\bar{e}), lower-level optimality $\|\nabla_y g(\mathbf{x}_k, \mathbf{y}_k)\|$, and upper-level objective function value $f(\mathbf{x}_k, \mathbf{y}_k)$ compared to other methods. To underscore the practical significance of the projection-free bilevel approach, we further conducted experiments on a more extensive dataset, with the results available in Appendix G.3.

5.2 Multi-Task Learning

In this section, we compare our IBCG method with other benchmarks for solving the Multi-Task Learning problem defined in (3). We use various datasets, including `bodyfat`, `housing`, `mg`, `mpg`, and `space-ga` from the LibSVM library Chang and Lin [CL11], treating each as the dataset corresponding to a distinct task. For each dataset $\mathcal{D}_i = (\mathbf{A}_i, \mathbf{b}_i)$, where $\mathbf{A}_i \in \mathbb{R}^{n_i \times d}$ and $\mathbf{b}_i \in \mathbb{R}^{n_i}$, we define its corresponding loss function as $L_i(w_i; \mathcal{D}_i) = \frac{1}{n_i} \|\mathbf{A}_i w_i - \mathbf{b}_i\|^2$. We assign 60% of the data points of each task as the training set $(\mathbf{A}_i^{\text{tr}}, \mathbf{b}_i^{\text{tr}})$, 20% as the validation set $(\mathbf{A}_i^{\text{val}}, \mathbf{b}_i^{\text{val}})$ and the rest as the test set $(\mathbf{A}_i^{\text{test}}, \mathbf{b}_i^{\text{test}})$. To evaluate our method’s efficacy, we compare it with a state-of-the-art projection-free method for constrained bilevel optimization problems namely SBFW, and excluding TTSA due to its frequent projections onto the constraint set, incurring substantial computational overhead – for the details of the experiment see Appendix G.4. Fig. 3 illustrates the performance of the two methods, showing our proposed method achieving faster convergence compared to the slower convergence rate of SBFW. To emphasize our method’s practical significance over SBFW, we also conducted this experiment by fixing the running time for both methods and observe that IBCG algorithm demonstrates rapid initial improvement as shown in Fig. 4. Furthermore, the comparison of test accuracy for the trained model with the algorithms and training datasets individually can be found in Appendix G.4.

6 Conclusion

In this paper, we focused on the constrained general bilevel optimization problem that appears in a wide range of applications. We introduced a novel single-loop projection-free method based on nested approximation techniques, which provides optimal convergence rate guarantees, matching the best-known complexity of projection-free algorithms for solving convex constrained single-level optimization problems. Specifically, we demonstrated that our method requires approximately $\tilde{\mathcal{O}}(\epsilon^{-1})$ iterations to find an ϵ -optimal solution when the hyper-objective function $\ell(x)$ is convex. For nonconvex $\ell(x)$, it takes approximately $\mathcal{O}(\epsilon^{-2})$ iterations to find an ϵ -stationary point. Our numerical results further underscored the superior performance of our IBCG algorithm compared to existing methods.

Acknowledgements

The research of N. Abolfazli and E. Yazdandoost Hamedani is supported by NSF Grant 2127696. The research of R. Jiang and A. Mokhtari is supported in part by NSF Grants 2127697, 2019844, and 2112471, ARO Grant W911NF2110226, the Machine Learning Lab (MLL) at UT Austin, and the Wireless Networking and Communications Group (WNCG) Industrial Affiliates Program.

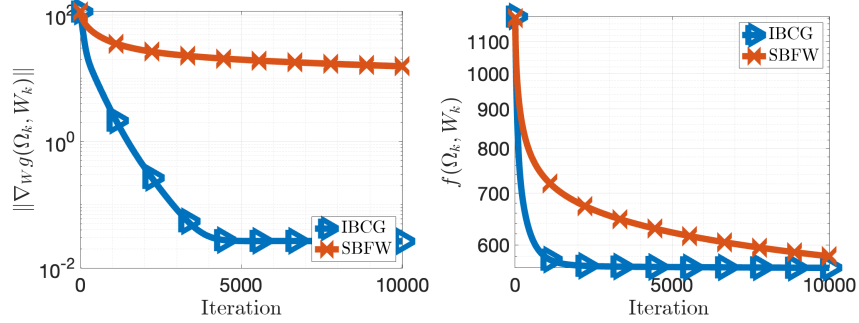


Figure 3: Performance of IBCG vs SBFW on problem (3) for real dataset1 . Plots from left to right: $\|\nabla_W g(\Omega_k, W_k)\|$, and $f(\Omega_k, W_k)$ in terms of number of iterations.

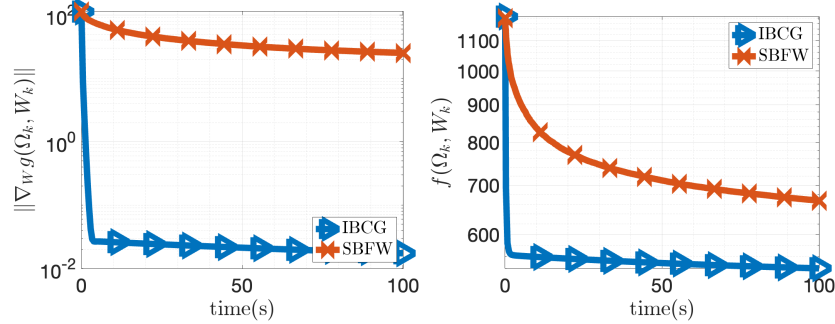


Figure 4: Performance of IBCG vs SBFW on problem (3) for real dataset1. Plots from left to right: $\|\nabla_W g(\Omega_k, W_k)\|$, and $f(\Omega_k, W_k)$ in terms of running time.

References

- [ABTR22] Zeeshan Akhtar, Amrit Singh Bedi, Srujan Teja Thomdapu, and Ketan Rajawat. “Projection-Free Stochastic Bi-Level Optimization”. In: *IEEE Transactions on Signal Processing* 70 (2022), pp. 6332–6347 (pages 2–6, 10, 11, 26, 27).
- [AM21] Michael Arbel and Julien Mairal. “Amortized implicit differentiation for stochastic bilevel optimization”. In: *arXiv preprint arXiv:2111.14580* (2021) (page 3).
- [BMK20] Zalán Borsos, Mojmir Mutny, and Andreas Krause. “Coresets via bilevel optimization for continual learning and streaming”. In: *Advances in Neural Information Processing Systems* 33 (2020), pp. 14879–14890 (page 2).
- [CL11] Chih-Chung Chang and Chih-Jen Lin. “LIBSVM: A library for support vector machines”. In: *ACM Transactions on Intelligent Systems and Technology* 2 (3 2011). Software available at <http://www.csie.ntu.edu.tw/~cjlin/libsvm>, 27:1–27:27 (pages 12, 30).
- [CXZ23] Lesi Chen, Jing Xu, and Jingzhao Zhang. “On Bilevel Optimization without Lower-level Strong Convexity”. In: *arXiv preprint arXiv:2301.00712* (2023) (page 4).
- [DAVM22] Mathieu Dagréou, Pierre Ablin, Samuel Vaiter, and Thomas Moreau. “A framework for bilevel optimization that enables stochastic and global variance reduction algorithms”. In: *Advances in Neural Information Processing Systems* 35 (2022), pp. 26698–26710 (page 4).

- [Dom12] Justin Domke. “Generic Methods for Optimization-Based Modeling”. In: *Proceedings of the Fifteenth International Conference on Artificial Intelligence and Statistics*. 2012, pp. 318–326 (page 2).
- [FMO20] Alireza Fallah, Aryan Mokhtari, and Asuman Ozdaglar. “Personalized federated learning with theoretical guarantees: A model-agnostic meta-learning approach”. In: *Advances in Neural Information Processing Systems* 33 (2020), pp. 3557–3568 (page 2).
- [FFSGP18a] L. Franceschi, P. Frasconi, S. Salzo, R. Grazzi, and M. Pontil. “Bilevel Programming for Hyperparameter Optimization and Meta-Learning”. In: *ICML*. 2018 (page 2).
- [FFSGP18b] Luca Franceschi, Paolo Frasconi, Saverio Salzo, Riccardo Grazzi, and Massimiliano Pontil. “Bilevel programming for hyperparameter optimization and meta-learning”. In: *International Conference on Machine Learning*. PMLR. 2018, pp. 1568–1577 (pages 2, 4).
- [FW56] Marguerite Frank and Philip Wolfe. “An algorithm for quadratic programming”. In: *Naval research logistics quarterly* 3.1-2 (1956), pp. 95–110 (page 2).
- [GW18] Saeed Ghadimi and Mengdi Wang. “Approximation methods for bilevel programming”. In: *arXiv preprint arXiv:1802.02246* (2018) (pages 2–4, 6, 7, 27).
- [GFCACG16] Stephen Gould, Basura Fernando, Anoop Cherian, Peter Anderson, Rodrigo Santa Cruz, and Edison Guo. “On differentiating parameterized argmin and argmax problems with application to bi-level optimization”. In: *arXiv preprint arXiv:1607.05447* (2016) (page 2).
- [GFPS20] Riccardo Grazzi, Luca Franceschi, Massimiliano Pontil, and Saverio Salzo. “On the iteration complexity of hypergradient computation”. In: *International Conference on Machine Learning*. PMLR. 2020, pp. 3748–3758 (page 2).
- [HJS92] Pierre Hansen, Brigitte Jaumard, and Gilles Savard. “New branch-and-bound rules for linear bilevel programming”. In: *SIAM Journal on scientific and Statistical Computing* 13.5 (1992), pp. 1194–1217 (page 2).
- [HWY20] Mingyi Hong, Hoi-To Wai, Zhaoran Wang, and Zhuoran Yang. “A two-timescale framework for bilevel optimization: Complexity analysis and application to actor-critic”. In: *arXiv preprint arXiv:2007.05170* (2020) (pages 2–4, 6, 10, 11, 26).
- [Jag13] Martin Jaggi. “Revisiting Frank-Wolfe: Projection-Free Sparse Convex Optimization”. In: *Proceedings of the 30th International Conference on Machine Learning*. 2013, pp. 427–435 (page 10).
- [JYL21] Kaiyi Ji, Junjie Yang, and Yingbin Liang. “Bilevel optimization: Convergence analysis and enhanced design”. In: *International Conference on Machine Learning*. 2021, pp. 4882–4892 (page 3).
- [KZHWY21] Prashant Khanduri, Siliang Zeng, Mingyi Hong, Hoi-To Wai, Zhaoran Wang, and Zhuoran Yang. “A near-optimal algorithm for stochastic bilevel optimization via double-momentum”. In: *Advances in neural information processing systems* 34 (2021), pp. 30271–30283 (page 3).
- [KKWN23] Jeongyeol Kwon, Dohyun Kwon, Stephen Wright, and Robert Nowak. “A Fully First-Order Method for Stochastic Bilevel Optimization”. In: *arXiv preprint arXiv:2301.10945* (2023) (pages 3, 4).

- [Lac16] Simon Lacoste-Julien. “Convergence rate of Frank-Wolfe for non-convex objectives”. In: *arXiv preprint arXiv:1607.00345* (2016) (page 3).
- [Lan13] Guanghui Lan. “The complexity of large-scale convex programming under a linear optimization oracle”. In: *arXiv preprint arXiv:1309.5550* (2013) (page 10).
- [LGH22] Junyi Li, Bin Gu, and Heng Huang. “A fully single loop algorithm for bilevel optimization without hessian inverse”. In: *Proceedings of the AAAI Conference on Artificial Intelligence*. Vol. 36. 7. 2022, pp. 7426–7434 (pages 3, 4).
- [LXFZYPUZ18] Renjie Liao, Yuwen Xiong, Ethan Fetaya, Lisa Zhang, KiJung Yoon, Xaq Pitkow, Raquel Urtasun, and Richard Zemel. “Reviving and improving recurrent back-propagation”. In: *International Conference on Machine Learning*. PMLR. 2018, pp. 3082–3091 (page 2).
- [LMYZZ20] Risheng Liu, Pan Mu, Xiaoming Yuan, Shangzhi Zeng, and Jin Zhang. “A generic first-order algorithmic framework for bi-level programming beyond lower-level singleton”. In: *International Conference on Machine Learning*. PMLR. 2020, pp. 6305–6315 (page 4).
- [LVD20] Jonathan Lorraine, Paul Vicol, and David Duvenaud. “Optimizing millions of hyperparameters by implicit differentiation”. In: *International Conference on Artificial Intelligence and Statistics*. PMLR. 2020, pp. 1540–1552 (page 2).
- [MDA15] Dougal Maclaurin, David Duvenaud, and Ryan Adams. “Gradient-based Hyperparameter Optimization through Reversible Learning”. In: *Proceedings of the 32nd International Conference on Machine Learning*. 2015, pp. 2113–2122 (page 2).
- [MD21] Andrew D McRae and Mark A Davenport. “Low-rank matrix completion and denoising under Poisson noise”. In: *Information and Inference: A Journal of the IMA* 10.2 (2021), pp. 697–720 (page 5).
- [MHK20] Aryan Mokhtari, Hamed Hassani, and Amin Karbasi. “Stochastic conditional gradient methods: From convex minimization to submodular maximization”. In: *The Journal of Machine Learning Research* 21.1 (2020), pp. 4232–4280 (page 11).
- [MOJ18] Aryan Mokhtari, Asuman Ozdaglar, and Ali Jadbabaie. “Escaping Saddle Points in Constrained Optimization”. In: *Advances in Neural Information Processing Systems (NIPS)* (2018) (page 3).
- [Moo10] Gregory M Moore. *Bilevel programming algorithms for machine learning model selection*. Rensselaer Polytechnic Institute, 2010 (page 2).
- [Nes18] Yurii Nesterov. *Lectures on convex optimization*. Vol. 137. Springer, 2018 (page 19).
- [Ped16] Fabian Pedregosa. “Hyperparameter optimization with approximate gradient”. In: *Proceedings of the 33rd International Conference on Machine Learning (ICML)*. 2016 (page 2).
- [RFKL19] Aravind Rajeswaran, Chelsea Finn, Sham M Kakade, and Sergey Levine. “Meta-learning with implicit gradients”. In: *Advances in neural information processing systems* 32 (2019) (pages 2, 4).
- [RSPS16] Sashank J Reddi, Suvrit Sra, Barnabás Póczos, and Alex Smola. “Stochastic frank-wolfe methods for nonconvex optimization”. In: *2016 54th annual Allerton conference on communication, control, and computing (Allerton)*. IEEE. 2016, pp. 1244–1251 (page 7).

- [SCHB19] Amirreza Shaban, Ching-An Cheng, Nathan Hatch, and Byron Boots. “Truncated back-propagation for bilevel optimization”. In: *The 22nd International Conference on Artificial Intelligence and Statistics*. PMLR. 2019, pp. 1723–1732 (pages 2, 4).
- [SC23] Han Shen and Tianyi Chen. “On penalty-based bilevel gradient descent method”. In: *arXiv preprint arXiv:2302.05185* (2023) (page 4).
- [SLZ05] Chenggen Shi, Jie Lu, and Guangquan Zhang. “An extended Kuhn–Tucker approach for linear bilevel programming”. In: *Applied Mathematics and Computation* 162.1 (2005), pp. 51–63 (page 2).
- [SJGL22] Daouda Sow, Kaiyi Ji, Ziwei Guan, and Yingbin Liang. “A constrained optimization approach to bilevel optimization with multiple inner minima”. In: *arXiv preprint arXiv:2203.01123* (2022) (page 4).
- [YLLJ23] Haikuo Yang, Luo Luo, Chris Junchi Li, and Michael I Jordan. “Accelerating Inexact HyperGradient Descent for Bilevel Optimization”. In: *arXiv preprint arXiv:2307.00126* (2023) (pages 3, 4).
- [YJL21] Junjie Yang, Kaiyi Ji, and Yingbin Liang. “Provably faster algorithms for bilevel optimization”. In: *Advances in Neural Information Processing Systems* 34 (2021), pp. 13670–13682 (pages 3, 6).
- [YH17] Tatsuya Yokota and Hidekata Hontani. “Simultaneous visual data completion and denoising based on tensor rank and total variation minimization and its primal-dual splitting algorithm”. In: *Proceedings of the IEEE Conference on Computer Vision and Pattern Recognition*. 2017, pp. 3732–3740 (pages 4, 5).
- [ZSMHK20] Mingrui Zhang, Zebang Shen, Aryan Mokhtari, Hamed Hassani, and Amin Karbasi. “One sample stochastic frank-wolfe”. In: *International Conference on Artificial Intelligence and Statistics*. PMLR. 2020, pp. 4012–4023 (page 7).
- [ZY14] Yu Zhang and Dit-Yan Yeung. “A regularization approach to learning task relationships in multitask learning”. In: *ACM Transactions on Knowledge Discovery from Data (TKDD)* 8.3 (2014), pp. 1–31 (page 5).

Appendix

In section **A**, we establish technical lemmas based on the assumptions considered in the paper. These lemmas characterize important properties of problem **1**. Notably, Lemma **2.1** is instrumental in understanding the properties associated with problem **1**. Moving on to section **B**, we present a series of lemmas essential for deriving the rate results of the proposed algorithm. Among them, Lemma **4.1** quantifies the error between the approximated direction F_k and $\nabla\ell(\mathbf{x}_k)$. This quantification plays a crucial role in establishing the one-step improvement lemma (see Lemma **B.4**). Next, we provide the proofs of Theorem **4.2** and Corollary **4.3** in sections **C** and **D**, respectively, that support the results presented in the paper for the convex scenario. Finally, in sections **E** and **F** we provide the proofs for Theorem **4.4** along with Corollary **4.5** for the nonconvex scenario.

A Supporting Lemmas

In this section, we provide detailed explanations and proofs for the lemmas supporting the main results of the paper.

A.1 Proof of Lemma **2.1**

(I) Recall that $\mathbf{y}^*(\mathbf{x})$ is the minimizer of the lower-level problem whose objective function is strongly convex, therefore,

$$\begin{aligned}\mu_g \|\mathbf{y}^*(\mathbf{x}) - \mathbf{y}^*(\bar{\mathbf{x}})\|^2 &\leq \langle \nabla_y g(\mathbf{x}, \mathbf{y}^*(\mathbf{x})) - \nabla_y g(\mathbf{x}, \mathbf{y}^*(\bar{\mathbf{x}})), \mathbf{y}^*(\mathbf{x}) - \mathbf{y}^*(\bar{\mathbf{x}}) \rangle \\ &= \langle \nabla_y g(\bar{\mathbf{x}}, \mathbf{y}^*(\bar{\mathbf{x}})) - \nabla_y g(\mathbf{x}, \mathbf{y}^*(\bar{\mathbf{x}})), \mathbf{y}^*(\mathbf{x}) - \mathbf{y}^*(\bar{\mathbf{x}}) \rangle\end{aligned}$$

Note that $\nabla_y g(\mathbf{x}, \mathbf{y}^*(\mathbf{x})) = \nabla_y g(\bar{\mathbf{x}}, \mathbf{y}^*(\bar{\mathbf{x}})) = 0$. Using the Cauchy-Schwartz inequality we have

$$\begin{aligned}\mu_g \|\mathbf{y}^*(\mathbf{x}) - \mathbf{y}^*(\bar{\mathbf{x}})\|^2 &\leq \|\nabla_y g(\bar{\mathbf{x}}, \mathbf{y}^*(\bar{\mathbf{x}})) - \nabla_y g(\mathbf{x}, \mathbf{y}^*(\bar{\mathbf{x}}))\| \|\mathbf{y}^*(\mathbf{x}) - \mathbf{y}^*(\bar{\mathbf{x}})\| \\ &\leq C_{yx}^g \|\mathbf{x} - \bar{\mathbf{x}}\| \|\mathbf{y}^*(\mathbf{x}) - \mathbf{y}^*(\bar{\mathbf{x}})\|\end{aligned}$$

where the last inequality is obtained by using the Assumption **2.2**. Therefore, we conclude that $\mu_g \|\mathbf{y}^*(\mathbf{x}) - \mathbf{y}^*(\bar{\mathbf{x}})\| \leq C_{yx}^g \|\mathbf{x} - \bar{\mathbf{x}}\|$ which leads to the desired result in part (I).

(II) We first show that the function $\mathbf{x} \mapsto \nabla_y f(\mathbf{x}, \mathbf{y}^*(\mathbf{x}))$ is Lipschitz continuous. To see this, note that for any $\mathbf{x}, \bar{\mathbf{x}} \in \mathcal{X}$, we have

$$\begin{aligned}\|\nabla_y f(\mathbf{x}, \mathbf{y}^*(\mathbf{x})) - \nabla_y f(\bar{\mathbf{x}}, \mathbf{y}^*(\bar{\mathbf{x}}))\| &\leq L_{yx}^f \|\mathbf{x} - \bar{\mathbf{x}}\| + L_{yy}^f \|\mathbf{y}^*(\mathbf{x}) - \mathbf{y}^*(\bar{\mathbf{x}})\| \\ &\leq \left(L_{yx}^f + \frac{L_{yy}^f C_{yx}^g}{\mu_g} \right) \|\mathbf{x} - \bar{\mathbf{x}}\|,\end{aligned}$$

where in the last inequality we used Lemma **2.1**-(I). Since \mathcal{X} is bounded, we also have $\|\mathbf{x} - \bar{\mathbf{x}}\| \leq D_{\mathcal{X}}$. Therefore, letting $\bar{\mathbf{x}} = \mathbf{x}^*$ in the above inequality and using the triangle inequality, we have

$$\|\nabla_y f(\mathbf{x}, \mathbf{y}^*(\mathbf{x}))\| \leq \left(L_{yx}^f + \frac{L_{yy}^f C_{yx}^g}{\mu_g} \right) D_{\mathcal{X}} + \|\nabla_y f(\mathbf{x}^*, \mathbf{y}^*(\mathbf{x}^*))\|.$$

Thus, we complete the proof by letting $C_y^f = \left(L_{yx}^f + \frac{L_{yy}^f C_{yx}^g}{\mu_g} \right) D_{\mathcal{X}} + \|\nabla_y f(\mathbf{x}^*, \mathbf{y}^*(\mathbf{x}^*))\|$.

Before proceeding to show the result of part (III) of Lemma **2.1**, we first establish an auxiliary lemma stated next.

Lemma A.1. *Under the premises of Lemma 2.1, we have that for any $\mathbf{x}, \bar{\mathbf{x}} \in \mathcal{X}$, $\|\mathbf{v}(\mathbf{x}) - \mathbf{v}(\bar{\mathbf{x}})\| \leq \mathbf{C}_v \|\mathbf{x} - \bar{\mathbf{x}}\|$ for some $\mathbf{C}_v \geq 0$.*

Proof. We start the proof by recalling that $\mathbf{v}(\mathbf{x}) = \nabla_{yy}^2 g(\mathbf{x}, \mathbf{y}^*(\mathbf{x}))^{-1} \nabla_y f(\mathbf{x}, \mathbf{y}^*(\mathbf{x}))$. Next, adding and subtracting $\nabla_{yy}^2 g(\mathbf{x}, \mathbf{y}^*(\mathbf{x})) \nabla_y f(\bar{\mathbf{x}}, \mathbf{y}^*(\bar{\mathbf{x}}))$ followed by a triangle inequality leads to,

$$\begin{aligned} & \|\mathbf{v}(\mathbf{x}) - \mathbf{v}(\bar{\mathbf{x}})\| \\ &= \|[\nabla_{yy}^2 g(\mathbf{x}, \mathbf{y}^*(\mathbf{x}))]^{-1} \nabla_y f(\mathbf{x}, \mathbf{y}^*(\mathbf{x})) - [\nabla_{yy}^2 g(\bar{\mathbf{x}}, \mathbf{y}^*(\bar{\mathbf{x}}))]^{-1} \nabla_y f(\bar{\mathbf{x}}, \mathbf{y}^*(\bar{\mathbf{x}}))\| \\ &\leq \|[\nabla_{yy}^2 g(\mathbf{x}, \mathbf{y}^*(\mathbf{x}))]^{-1} (\nabla_y f(\mathbf{x}, \mathbf{y}^*(\mathbf{x})) - \nabla_y f(\bar{\mathbf{x}}, \mathbf{y}^*(\bar{\mathbf{x}})))\| + \|([\nabla_{yy}^2 g(\mathbf{x}, \mathbf{y}^*(\mathbf{x}))]^{-1} \\ &\quad - [\nabla_{yy}^2 g(\bar{\mathbf{x}}, \mathbf{y}^*(\bar{\mathbf{x}}))]^{-1}) \nabla_y f(\bar{\mathbf{x}}, \mathbf{y}^*(\bar{\mathbf{x}}))\| \\ &\leq \frac{1}{\mu_g} (L_{yx}^f \|\mathbf{x} - \bar{\mathbf{x}}\| + L_{yy}^f \|\mathbf{y}^*(\mathbf{x}) - \mathbf{y}^*(\bar{\mathbf{x}})\|) + C_y^f \|[\nabla_{yy}^2 g(\mathbf{x}, \mathbf{y}^*(\mathbf{x}))]^{-1} - [\nabla_{yy}^2 g(\bar{\mathbf{x}}, \mathbf{y}^*(\bar{\mathbf{x}}))]^{-1}\|, \end{aligned} \quad (10)$$

where in the last inequality we used Assumptions 2.1 and 2.2-(iii) along with the premises of Lemma 2.1-(II). Moreover, for any invertible matrices H_1 and H_2 , we have that

$$\|H_2^{-1} - H_1^{-1}\| = \|H_1^{-1}(H_1 - H_2)H_2^{-1}\| \leq \|H_1^{-1}\| \|H_2^{-1}\| \|H_1 - H_2\|. \quad (11)$$

Therefore, using the result of Lemma 2.1-(I) and (11) we can further bound inequality (10) as follows,

$$\begin{aligned} & \|\mathbf{v}(\mathbf{x}) - \mathbf{v}(\bar{\mathbf{x}})\| \\ &\leq \frac{1}{\mu_g} (L_{yx}^f \|\mathbf{x} - \bar{\mathbf{x}}\| + L_{yy}^f \mathbf{L}_y \|\mathbf{x} - \bar{\mathbf{x}}\|) + C_y^f \|[\nabla_{yy}^2 g(\mathbf{x}, \mathbf{y}^*(\mathbf{x}))]^{-1} - [\nabla_{yy}^2 g(\bar{\mathbf{x}}, \mathbf{y}^*(\bar{\mathbf{x}}))]^{-1}\| \\ &\leq \frac{1}{\mu_g} (L_{yx}^f + L_{yy}^f \mathbf{L}_y) \|\mathbf{x} - \bar{\mathbf{x}}\| + \frac{C_y^f}{\mu_g^2} L_{yy}^g (\|\mathbf{x} - \bar{\mathbf{x}}\| + \|\mathbf{y}^*(\mathbf{x}) - \mathbf{y}^*(\bar{\mathbf{x}})\|) \\ &= \left(\frac{L_{yx}^f + L_{yy}^f \mathbf{L}_y}{\mu_g} + \frac{C_y^f L_{yy}^g}{\mu_g^2} (1 + \mathbf{L}_y) \right) \|\mathbf{x} - \bar{\mathbf{x}}\|. \end{aligned}$$

The result follows by letting $\mathbf{C}_v = \frac{L_{yx}^f + L_{yy}^f \mathbf{L}_y}{\mu_g} + \frac{C_y^f L_{yy}^g}{\mu_g^2} (1 + \mathbf{L}_y)$. \square

(III) We start proving this part using the definition of $\nabla \ell(\mathbf{x})$ stated in (6a). Utilizing the triangle inequality we obtain

$$\begin{aligned} & \|\nabla \ell(\mathbf{x}) - \nabla \ell(\bar{\mathbf{x}})\| \\ &= \|\nabla_x f(\mathbf{x}, \mathbf{y}^*(\mathbf{x})) - \nabla_{yx}^2 g(\mathbf{x}, \mathbf{y}^*(\mathbf{x})) \mathbf{v}(\mathbf{x}) - (\nabla_x f(\bar{\mathbf{x}}, \mathbf{y}^*(\bar{\mathbf{x}})) - \nabla_{yx}^2 g(\bar{\mathbf{x}}, \mathbf{y}^*(\bar{\mathbf{x}})) \mathbf{v}(\bar{\mathbf{x}}))\| \\ &\leq \|\nabla_x f(\mathbf{x}, \mathbf{y}^*(\mathbf{x})) - \nabla_x f(\bar{\mathbf{x}}, \mathbf{y}^*(\bar{\mathbf{x}}))\| + \|[\nabla_{yx}^2 g(\bar{\mathbf{x}}, \mathbf{y}^*(\bar{\mathbf{x}})) \mathbf{v}(\bar{\mathbf{x}}) - \nabla_{yx}^2 g(\bar{\mathbf{x}}, \mathbf{y}^*(\bar{\mathbf{x}})) \mathbf{v}(\mathbf{x})] \\ &\quad + [\nabla_{yx}^2 g(\bar{\mathbf{x}}, \mathbf{y}^*(\bar{\mathbf{x}})) \mathbf{v}(\mathbf{x}) - \nabla_{yx}^2 g(\mathbf{x}, \mathbf{y}^*(\mathbf{x})) \mathbf{v}(\mathbf{x})]\| \end{aligned} \quad (12)$$

where the second term of the RHS follows from adding and subtracting the term $\nabla_{yx}^2 g(\bar{\mathbf{x}}, \mathbf{y}^*(\bar{\mathbf{x}})) \mathbf{v}(\mathbf{x})$. Next, from Assumptions 2.1-(i) and 2.2-(v) together with the triangle inequality application we conclude that

$$\begin{aligned} \|\nabla \ell(\mathbf{x}) - \nabla \ell(\bar{\mathbf{x}})\| &\leq L_{xx}^f \|\mathbf{x} - \bar{\mathbf{x}}\| + L_{xy}^f \|\mathbf{y}^*(\mathbf{x}) - \mathbf{y}^*(\bar{\mathbf{x}})\| + C_{yx}^g \|\mathbf{v}(\bar{\mathbf{x}}) - \mathbf{v}(\mathbf{x})\| \\ &\quad + \frac{C_y^f}{\mu_g} \|\nabla_{yx}^2 g(\bar{\mathbf{x}}, \mathbf{y}^*(\bar{\mathbf{x}})) - \nabla_{yx}^2 g(\mathbf{x}, \mathbf{y}^*(\mathbf{x}))\| \end{aligned} \quad (13)$$

It should be that in the last inequality, we use the fact that $\|\mathbf{v}(\mathbf{x})\| = \|[\nabla_{yy}^2 g(\mathbf{x}, \mathbf{y}^*(\mathbf{x}))]^{-1} \nabla_y f(\mathbf{x}, \mathbf{y}^*(\mathbf{x}))\| \leq \frac{C_y^f}{\mu_g}$. Combining the result of Lemma 2.1 part (I) and (II) with the Assumption 2.2-(iv) leads to

$$\begin{aligned}
\|\nabla \ell(\mathbf{x}) - \nabla \ell(\bar{\mathbf{x}})\| &\leq L_{xx}^f \|\mathbf{x} - \bar{\mathbf{x}}\| + L_{xy}^f \mathbf{L}_y \|\mathbf{x} - \bar{\mathbf{x}}\| + C_{yx}^g \mathbf{C}_v \|\mathbf{x} - \bar{\mathbf{x}}\| \\
&\quad + \frac{C_y^f}{\mu_g} L_{yx}^g (\|\mathbf{x} - \bar{\mathbf{x}}\| + \|\mathbf{y}^*(\mathbf{x}) - \mathbf{y}^*(\bar{\mathbf{x}})\|) \\
&\leq L_{xx}^f \|\mathbf{x} - \bar{\mathbf{x}}\| + L_{xy}^f \mathbf{L}_y \|\mathbf{x} - \bar{\mathbf{x}}\| + C_{yx}^g \mathbf{C}_v \|\mathbf{x} - \bar{\mathbf{x}}\| \\
&\quad + \frac{C_y^f}{\mu_g} L_{yx}^g (\|\mathbf{x} - \bar{\mathbf{x}}\| + \mathbf{L}_y \|\mathbf{x} - \bar{\mathbf{x}}\|) \\
&\leq (L_{xx}^f + L_{xy}^f \mathbf{L}_y + C_{yx}^g \mathbf{C}_v + \frac{C_y^f}{\mu_g} L_{yx}^g (1 + \mathbf{L}_y)) \|\mathbf{x} - \bar{\mathbf{x}}\| \tag{14}
\end{aligned}$$

The desired result can be obtained by letting $\mathbf{L}_\ell = L_{xx}^f + L_{xy}^f \mathbf{L}_y + C_{yx}^g \mathbf{C}_v + \frac{C_y^f}{\mu_g} L_{yx}^g (1 + \mathbf{L}_y)$. \square

B Required Lemmas for Theorems 4.2 and 4.4

Before we proceed to the proofs of Theorems 4.2 and 4.4, we present the following technical lemmas which quantify the error between the approximated solution \mathbf{y}_k and $\mathbf{y}^*(\mathbf{x}_k)$, as well as between \mathbf{w}_{k+1} and $\mathbf{v}(\mathbf{x}_k)$.

Lemma B.1. *Suppose Assumption 2.2 holds. Let $\{(\mathbf{x}_k, \mathbf{y}_k)\}_{k \geq 0}$ be the sequence generated by Algorithm 1, such that $\alpha = 2/(\mu_g + L_g)$. Then, for any $k \geq 0$*

$$\|\mathbf{y}_k - \mathbf{y}^*(\mathbf{x}_k)\| \leq \beta^k \|\mathbf{y}_0 - \mathbf{y}^*(\mathbf{x}_0)\| + \mathbf{L}_y D_{\mathcal{X}} \sum_{i=0}^{k-1} \gamma_i \beta^{k-i}, \tag{15}$$

where $\beta \triangleq (L_g - \mu_g)/(L_g + \mu_g)$.

Proof. We begin the proof by characterizing the one-step progress of the lower-level iterate sequence $\{\mathbf{y}_k\}_k$. Indeed, at iteration k we aim to approximate $\mathbf{y}^*(\mathbf{x}_{k+1}) = \operatorname{argmin}_{\mathbf{y}} g(\mathbf{x}_{k+1}, \mathbf{y})$. According to the update of \mathbf{y}_{k+1} we observe that

$$\begin{aligned}
\|\mathbf{y}_{k+1} - \mathbf{y}^*(\mathbf{x}_{k+1})\|^2 &= \|\mathbf{y}_k - \mathbf{y}^*(\mathbf{x}_{k+1}) - \alpha \nabla_y g(\mathbf{x}_{k+1}, \mathbf{y}_k)\|^2 \\
&= \|\mathbf{y}_k - \mathbf{y}^*(\mathbf{x}_{k+1})\|^2 - 2\alpha \langle \nabla_y g(\mathbf{x}_{k+1}, \mathbf{y}_k), \mathbf{y}_k - \mathbf{y}^*(\mathbf{x}_{k+1}) \rangle \\
&\quad + \alpha^2 \|\nabla_y g(\mathbf{x}_{k+1}, \mathbf{y}_k)\|^2. \tag{16}
\end{aligned}$$

Moreover, from Assumption 2.2 and following Theorem 2.1.12 in Nesterov [Nes18], we have that

$$\langle \nabla_y g(\mathbf{x}_{k+1}, \mathbf{y}_k), \mathbf{y}_k - \mathbf{y}^*(\mathbf{x}_{k+1}) \rangle \geq \frac{\mu_g L_g}{\mu_g + L_g} \|\mathbf{y}_k - \mathbf{y}^*(\mathbf{x}_{k+1})\|^2 + \frac{1}{\mu_g + L_g} \|\nabla_y g(\mathbf{x}_{k+1}, \mathbf{y}_k)\|^2 \tag{17}$$

The inequality in (16) together with (17) imply that

$$\begin{aligned}
\|\mathbf{y}_{k+1} - \mathbf{y}^*(\mathbf{x}_{k+1})\|^2 &\leq \|\mathbf{y}_k - \mathbf{y}^*(\mathbf{x}_{k+1})\|^2 - \frac{2\alpha \mu_g L_g}{\mu_g + L_g} \|\mathbf{y}_k - \mathbf{y}^*(\mathbf{x}_{k+1})\|^2 \\
&\quad + \left(\alpha^2 - \frac{2\alpha}{\mu_g + L_g} \right) \|\nabla_y g(\mathbf{x}_{k+1}, \mathbf{y}_k)\|^2. \tag{18}
\end{aligned}$$

Setting the step-size $\alpha = \frac{2}{\mu_g + L_g}$ in (18) leads to

$$\|\mathbf{y}_{k+1} - \mathbf{y}^*(\mathbf{x}_{k+1})\|^2 \leq \left(\frac{\mu_g - L_g}{\mu_g + L_g}\right)^2 \|\mathbf{y}_k - \mathbf{y}^*(\mathbf{x}_{k+1})\|^2 \quad (19)$$

Next, recall that $\beta = (L_g - \mu_g)/(L_g + \mu_g)$. Using the triangle inequality and Part (I) of Lemma 2.1 we conclude that

$$\begin{aligned} \|\mathbf{y}_{k+1} - \mathbf{y}^*(\mathbf{x}_{k+1})\| &\leq \beta \|\mathbf{y}_k - \mathbf{y}^*(\mathbf{x}_{k+1})\| \\ &\leq \beta \left[\|\mathbf{y}_k - \mathbf{y}^*(\mathbf{x}_k)\| + \|\mathbf{y}^*(\mathbf{x}_k) - \mathbf{y}^*(\mathbf{x}_{k+1})\| \right] \\ &\leq \beta \left[\|\mathbf{y}_k - \mathbf{y}^*(\mathbf{x}_k)\| + \mathbf{L}_y \|\mathbf{x}_k - \mathbf{x}_{k+1}\| \right]. \end{aligned} \quad (20)$$

Moreover, from the update of \mathbf{x}_{k+1} in Algorithm 1 and boundedness of \mathcal{X} we have that $\|\mathbf{x}_{k+1} - \mathbf{x}_k\| \leq \gamma_k D_{\mathcal{X}}$. Therefore, using this inequality within (20) leads to

$$\|\mathbf{y}_{k+1} - \mathbf{y}^*(\mathbf{x}_{k+1})\| \leq \beta \|\mathbf{y}_k - \mathbf{y}^*(\mathbf{x}_k)\| + \beta \gamma_k \mathbf{L}_y D_{\mathcal{X}}.$$

Finally, the desired result can be deduced from the above inequality recursively. \square

Previously, in Lemma B.1 we quantified how close the approximation \mathbf{y}_k is from the optimal solution $\mathbf{y}^*(\mathbf{x}_k)$ of the inner problem. Now, in the following Lemma, we will find an upper bound for the error of approximating $\mathbf{v}(\mathbf{x}_k)$ via \mathbf{w}_{k+1} .

Lemma B.2. *Let $\{(\mathbf{x}_k, \mathbf{w}_k)\}_{k \geq 0}$ be the sequence generated by Algorithm 1, such that $\gamma_k = \gamma$. Define $\rho_k \triangleq (1 - \eta_k \mu_g)$ and $\mathbf{C}_1 \triangleq L_{yy}^g \frac{C_y^f}{\mu_g} + L_{yy}^f$. Under Assumptions 2.1 and 2.2 we have that for any $k \geq 0$,*

$$\|\mathbf{w}_{k+1} - \mathbf{v}(\mathbf{x}_k)\| \leq \rho_k \|\mathbf{w}_k - \mathbf{v}(\mathbf{x}_{k-1})\| + \rho_k \mathbf{C}_v \gamma D_{\mathcal{X}} + \eta_k \mathbf{C}_1 \left(\beta^k D_0^y + \mathbf{L}_y \gamma \frac{\beta}{1 - \beta} D_{\mathcal{X}} \right). \quad (21)$$

Proof. From the optimality condition of (7) one can easily verify that $\mathbf{v}(\mathbf{x}_k) = \mathbf{v}(\mathbf{x}_k) - \eta_k (\nabla_{yy}^2 g(\mathbf{x}_k, \mathbf{y}^*(\mathbf{x}_k)) \mathbf{v}(\mathbf{x}_k) - \nabla_y f(\mathbf{x}_k, \mathbf{y}^*(\mathbf{x}_k)))$. Now using definition of \mathbf{w}_{k+1} we can write

$$\begin{aligned} \|\mathbf{w}_{k+1} - \mathbf{v}(\mathbf{x}_k)\| &= \left\| \left(\mathbf{w}_k - \eta_k (\nabla_{yy}^2 g(\mathbf{x}_k, \mathbf{y}_k) \mathbf{w}_k - \nabla_y f(\mathbf{x}_k, \mathbf{y}_k)) \right) - \left(\mathbf{v}(\mathbf{x}_k) \right. \right. \\ &\quad \left. \left. - \eta_k (\nabla_{yy}^2 g(\mathbf{x}_k, \mathbf{y}^*(\mathbf{x}_k)) \mathbf{v}(\mathbf{x}_k) - \nabla_y f(\mathbf{x}_k, \mathbf{y}^*(\mathbf{x}_k))) \right) \right\| \\ &= \left\| \left(I - \eta_k \nabla_{yy}^2 g(\mathbf{x}_k, \mathbf{y}_k) \right) (\mathbf{w}_k - \mathbf{v}(\mathbf{x}_k)) - \eta_k \left(\nabla_{yy}^2 g(\mathbf{x}_k, \mathbf{y}_k) \right. \right. \\ &\quad \left. \left. - \nabla_{yy}^2 g(\mathbf{x}_k, \mathbf{y}^*(\mathbf{x}_k)) \right) \mathbf{v}(\mathbf{x}_k) + \eta_k \left(\nabla_y f(\mathbf{x}_k, \mathbf{y}^*(\mathbf{x}_k)) - \nabla_y f(\mathbf{x}_k, \mathbf{y}_k) \right) \right\|, \end{aligned} \quad (22)$$

where the last equality is obtained by adding and subtracting the term $(I - \eta_k \nabla_{yy}^2 g(\mathbf{x}_k, \mathbf{y}_k)) \mathbf{v}(\mathbf{x}_k)$. Next, using Assumptions 2.1 and 2.2 along with the application of the triangle inequality we obtain

$$\begin{aligned} \|\mathbf{w}_{k+1} - \mathbf{v}(\mathbf{x}_k)\| &\leq (1 - \eta_k \mu_g) \|\mathbf{w}_k - \mathbf{v}(\mathbf{x}_k)\| + \eta_k L_{yy}^g \|\mathbf{y}_k - \mathbf{y}^*(\mathbf{x}_k)\| \|\mathbf{v}(\mathbf{x}_k)\| \\ &\quad + \eta_k L_{yy}^f \|\mathbf{y}_k - \mathbf{y}^*(\mathbf{x}_k)\|. \end{aligned} \quad (23)$$

Note that $\|\mathbf{v}(\mathbf{x}_k)\| = \|[\nabla_{yy}^2 g(\mathbf{x}, \mathbf{y}^*(\mathbf{x}))]^{-1} \nabla_y f(\mathbf{x}, \mathbf{y}^*(\mathbf{x}))\| \leq \frac{C_y^f}{\mu_g}$. Now, by adding and subtracting $\mathbf{v}(\mathbf{x}_{k-1})$ to the term $\|\mathbf{w}_k - \mathbf{v}(\mathbf{x}_k)\|$ followed by triangle inequality application we can conclude that

$$\begin{aligned} \|\mathbf{w}_{k+1} - \mathbf{v}(\mathbf{x}_k)\| &\leq (1 - \eta_k \mu_g) \|\mathbf{w}_k - \mathbf{v}(\mathbf{x}_{k-1})\| + (1 - \eta_k \mu_g) \|\mathbf{v}(\mathbf{x}_{k-1}) - \mathbf{v}(\mathbf{x}_k)\| \\ &\quad + \eta_k \left(L_{yy}^g \frac{C_y^f}{\mu_g} + L_{yy}^f \right) \|\mathbf{y}_k - \mathbf{y}^*(\mathbf{x}_k)\|. \end{aligned} \quad (24)$$

Therefore, using the result of Lemma B.1, we can further bound inequality (24) as follows

$$\begin{aligned} \|\mathbf{w}_{k+1} - \mathbf{v}(\mathbf{x}_k)\| &\leq (1 - \eta_k \mu_g) \|\mathbf{w}_k - \mathbf{v}(\mathbf{x}_{k-1})\| + (1 - \eta_k \mu_g) \mathbf{C}_v \|\mathbf{x}_{k-1} - \mathbf{x}_k\| \\ &\quad + \eta_k \mathbf{C}_1 \|\mathbf{y}_k - \mathbf{y}^*(\mathbf{x}_k)\| \\ &\leq \rho_k \|\mathbf{w}_k - \mathbf{v}(\mathbf{x}_{k-1})\| + \rho_k \mathbf{C}_v \gamma D_{\mathcal{X}} + \eta_k \mathbf{C}_1 (\beta^k D_0^y + \mathbf{L}_y \gamma \frac{\beta}{1 - \beta} D_{\mathcal{X}}) \end{aligned} \quad (25)$$

where the last inequality follows from the boundedness assumption of set \mathcal{X} , recalling that $D_0^y = \|\mathbf{y}_0 - \mathbf{y}^*(\mathbf{x}_0)\|$, and the fact that $\sum_{i=0}^{k-1} \beta^{k-i} \leq \frac{\beta}{1-\beta}$. \square

Lemma B.3. *Let $\{(\mathbf{x}_k, \mathbf{w}_k)\}_{k \geq 0}$ be the sequence generated by Algorithm 1 with step-size $\eta_k = \eta < \frac{1-\beta}{\mu_g}$ where β is defined in Lemma B.1. Suppose that Assumption 2.2 holds and $\mathbf{v}(\mathbf{x}_{-1}) = \mathbf{v}(\mathbf{x}_0)$, then for any $K \geq 1$,*

$$\|\mathbf{w}_K - \mathbf{v}(\mathbf{x}_{K-1})\| \leq \rho^K \|\mathbf{w}_0 - \mathbf{v}(\mathbf{x}_0)\| + \frac{\gamma \rho \mathbf{C}_v D_{\mathcal{X}}}{1 - \rho} + \frac{\eta \mathbf{C}_1 D_0^y \rho^{K+1}}{\rho - \beta} + \frac{\gamma \eta \beta \mathbf{C}_1 \mathbf{L}_y D_{\mathcal{X}}}{(1 - \rho)(1 - \beta)}, \quad (26)$$

where $\rho \triangleq 1 - \eta \mu_g$.

Proof. Applying the result of Lemma B.2 recursively for $k = 0$ to $K - 1$, one can conclude that

$$\begin{aligned} \|\mathbf{w}_K - \mathbf{v}(\mathbf{x}_{K-1})\| &\leq \rho^K \|\mathbf{w}_0 - \mathbf{v}(\mathbf{x}_0)\| + \mathbf{C}_v \gamma D_{\mathcal{X}} \sum_{i=1}^K \rho^i + \eta \mathbf{C}_1 \sum_{i=0}^K (\beta^i D_0^y + \gamma \mathbf{L}_y D_{\mathcal{X}} \frac{\beta}{1 - \beta}) \rho^{K-i} \\ &\leq \rho^K \|\mathbf{w}_0 - \mathbf{v}(\mathbf{x}_0)\| + \frac{\rho}{1 - \rho} \mathbf{C}_v \gamma D_{\mathcal{X}} + \eta \mathbf{C}_1 D_0^y \left(\sum_{i=0}^K \beta^i \rho^{K-i} \right) \\ &\quad + \frac{\gamma \eta \beta \mathbf{C}_1 \mathbf{L}_y D_{\mathcal{X}}}{1 - \beta} \sum_{i=0}^K \rho^{K-i}, \end{aligned} \quad (27)$$

where the last inequality is obtained by noting that $\sum_{i=1}^K \rho^i \leq \frac{\rho}{1-\rho}$. Finally, the choice $\eta < \frac{1-\beta}{\mu_g}$ implies that $\beta < \rho$, hence, $\sum_{i=0}^K (\frac{\beta}{\rho})^i \leq \frac{\rho}{\rho-\beta}$ which leads to the desired result. \square

B.1 Proof of Lemma 4.1

We begin the proof by considering the definition of $\nabla \ell(\mathbf{x}_k)$ and F_k followed by a triangle inequality to obtain

$$\begin{aligned} \|\nabla \ell(\mathbf{x}_k) - F_k\| &\leq \|\nabla_x f(\mathbf{x}_k, \mathbf{y}^*(\mathbf{x}_k)) - \nabla_x f(\mathbf{x}_k, \mathbf{y}_k)\| \\ &\quad + \|\nabla_{yx}^2 g(\mathbf{x}_k, \mathbf{y}_k) \mathbf{w}_{k+1} - \nabla_{yx}^2 g(\mathbf{x}_k, \mathbf{y}^*(\mathbf{x}_k)) \mathbf{v}(\mathbf{x}_k)\| \end{aligned} \quad (28)$$

Combining Assumption 2.1-(i) together with adding and subtracting $\nabla_{yx}^2 g(\mathbf{x}_k, \mathbf{y}_k) \mathbf{v}(\mathbf{x}_k)$ to the second term of RHS lead to

$$\begin{aligned} \|\nabla \ell(\mathbf{x}_k) - F_k\| &\leq L_{xy}^f \|\mathbf{y}_k - \mathbf{y}^*(\mathbf{x}_k)\| + \|\nabla_{yx}^2 g(\mathbf{x}_k, \mathbf{y}_k) (\mathbf{w}_{k+1} - \mathbf{v}(\mathbf{x}_k)) + (\nabla_{yx}^2 g(\mathbf{x}_k, \mathbf{y}_k) \\ &\quad - \nabla_{yx}^2 g(\mathbf{x}_k, \mathbf{y}^*(\mathbf{x}_k))) \mathbf{v}(\mathbf{x}_k)\| \\ &\leq L_{xy}^f \|\mathbf{y}_k - \mathbf{y}^*(\mathbf{x}_k)\| + C_{yx}^g \|\mathbf{w}_{k+1} - \mathbf{v}(\mathbf{x}_k)\| + L_{yx}^g \frac{C_y^f}{\mu_g} \|\mathbf{y}_k - \mathbf{y}^*(\mathbf{x}_k)\| \end{aligned} \quad (29)$$

where the last inequality is obtained using Assumption 2.2 and the triangle inequality. Next, utilizing Lemma B.1 and B.3 we can further provide upper-bounds for the term in RHS of (29) as follows

$$\begin{aligned} \|\nabla \ell(\mathbf{x}_k) - F_k\| &\leq \mathbf{C}_2 (\beta^k D_0^y + \frac{\gamma \beta \mathbf{L}_y D_{\mathcal{X}}}{1 - \beta}) + C_{yx}^g (\rho^{k+1} \|\mathbf{w}_0 - \mathbf{v}(\mathbf{x}_0)\| + \frac{\gamma \rho \mathbf{C}_v D_{\mathcal{X}}}{1 - \rho} \\ &\quad + \frac{\eta \mathbf{C}_1 D_0^y \rho^{k+2}}{\rho - \beta} + \frac{\gamma \eta \beta \mathbf{C}_1 \mathbf{L}_y D_{\mathcal{X}}}{(1 - \rho)(1 - \beta)}). \end{aligned}$$

□

B.2 Improvement in one step

In the following, we characterize the improvement of the objective function $\ell(\mathbf{x})$ after taking one step of Algorithm 1.

Lemma B.4. *Let $\{\mathbf{x}_k\}_{k=0}^K$ be the sequence generated by Algorithm 1. Suppose Assumptions 2.1 and 2.2 hold and $\gamma_k = \gamma$, then for any $k \geq 0$ we have*

$$\begin{aligned} \ell(\mathbf{x}_{k+1}) &\leq \ell(\mathbf{x}_k) - \gamma \mathcal{G}(\mathbf{x}_k) + \gamma \mathbf{C}_2 \beta^k D_0^y D_{\mathcal{X}} + \frac{\gamma^2 \mathbf{C}_2 D_{\mathcal{X}}^2 \mathbf{L}_y \beta}{1 - \beta} + C_{yx}^g \left[\gamma D_{\mathcal{X}} \rho^{k+1} \|\mathbf{w}_0 - \mathbf{v}(\mathbf{x}_0)\| \right. \\ &\quad \left. + \frac{\gamma^2 D_{\mathcal{X}}^2 \rho \mathbf{C}_v}{1 - \rho} + \frac{\gamma D_{\mathcal{X}} D_0^y \mathbf{C}_1 \eta \rho^{k+2}}{\rho - \beta} + \frac{\gamma^2 D_{\mathcal{X}}^2 \mathbf{L}_y \mathbf{C}_1 \beta \eta}{(1 - \beta)(1 - \rho)} \right] + \frac{1}{2} \mathbf{L}_{\ell} \gamma^2 D_{\mathcal{X}}^2. \end{aligned} \quad (30)$$

Proof. Note that according to Lemma 2.1-(III), $\ell(\cdot)$ has a Lipschitz continuous gradient which implies that

$$\begin{aligned} \ell(\mathbf{x}_{k+1}) &\leq \ell(\mathbf{x}_k) + \gamma \langle \nabla \ell(\mathbf{x}_k), \mathbf{s}_k - \mathbf{x}_k \rangle + \frac{1}{2} \mathbf{L}_{\ell} \gamma^2 \|\mathbf{s}_k - \mathbf{x}_k\|^2 \\ &= \ell(\mathbf{x}_k) + \gamma \langle F_k, \mathbf{s}_k - \mathbf{x}_k \rangle + \gamma \langle \nabla \ell(\mathbf{x}_k) - F_k, \mathbf{s}_k - \mathbf{x}_k \rangle + \frac{1}{2} \mathbf{L}_{\ell} \gamma^2 \|\mathbf{s}_k - \mathbf{x}_k\|^2, \end{aligned} \quad (31)$$

where the last inequality follows from adding and subtracting the term $\gamma \langle F_k, \mathbf{s}_k - \mathbf{x}_k \rangle$ to the RHS. Define $\mathbf{s}'_k = \operatorname{argmax}_{\mathbf{s} \in \mathcal{X}} \{\langle \nabla \ell(\mathbf{x}_k), \mathbf{x}_k - \mathbf{s} \rangle\}$ and observe that $\mathcal{G}(\mathbf{x}_k) = \langle \nabla \ell(\mathbf{x}_k), \mathbf{x}_k - \mathbf{s}'_k \rangle$ by Definition 2.1. Using the definition of \mathbf{s}_k , we can immediately observe that

$$\begin{aligned} \langle F_k, \mathbf{s}_k - \mathbf{x}_k \rangle &= \min_{\mathbf{s} \in \mathcal{X}} \langle F_k, \mathbf{s} - \mathbf{x}_k \rangle \\ &\leq \langle F_k, \mathbf{s}'_k - \mathbf{x}_k \rangle \\ &= \langle \nabla \ell(\mathbf{x}_k), \mathbf{s}'_k - \mathbf{x}_k \rangle + \langle F_k - \nabla \ell(\mathbf{x}_k), \mathbf{s}'_k - \mathbf{x}_k \rangle \\ &= -\mathcal{G}(\mathbf{x}_k) + \langle F_k - \nabla \ell(\mathbf{x}_k), \mathbf{s}'_k - \mathbf{x}_k \rangle. \end{aligned} \quad (32)$$

Next, combining (31) with (32) followed by the Cauchy-Schwartz inequality leads to

$$\ell(\mathbf{x}_{k+1}) \leq \ell(\mathbf{x}_k) - \gamma \mathcal{G}(\mathbf{x}_k) + \gamma \|\nabla \ell(\mathbf{x}_k) - F_k\| \|\mathbf{s}_k - \mathbf{s}'_k\| + \frac{1}{2} \mathbf{L}_\ell \gamma^2 \|\mathbf{s}_k - \mathbf{x}_k\|^2. \quad (33)$$

Finally, using the result of the Lemma 4.1 together with the boundedness assumption of set \mathcal{X} we conclude the desired result. \square

C Proof of Theorem 4.2

Since ℓ is convex, from the definition of $\mathcal{G}(\mathbf{x}_k)$ in (4) we have

$$\mathcal{G}(\mathbf{x}_k) = \max_{\mathbf{s} \in \mathcal{X}} \{\langle \nabla \ell(\mathbf{x}_k), \mathbf{x}_k - \mathbf{s} \rangle\} \geq \langle \nabla \ell(\mathbf{x}_k), \mathbf{x}_k - \mathbf{x}^* \rangle \geq \ell(\mathbf{x}_k) - \ell(\mathbf{x}^*). \quad (34)$$

We assume a fixed step-size in Theorem 4.2 and we set $\gamma_k = \gamma$. Combining the result of Lemma B.4 with (34) leads to

$$\begin{aligned} \ell(\mathbf{x}_{k+1}) \leq & \ell(\mathbf{x}_k) - \gamma(\ell(\mathbf{x}_k) - \ell(\mathbf{x}^*)) + \gamma \mathbf{C}_2 \beta^k D_0^y D_{\mathcal{X}} + \frac{\gamma^2 \mathbf{C}_2 D_{\mathcal{X}}^2 \mathbf{L}_y \beta}{1 - \beta} + C_{yx}^g \left[\gamma D_{\mathcal{X}} \rho^{k+1} \|\mathbf{w}_0 - \mathbf{v}(\mathbf{x}_0)\| \right. \\ & \left. + \frac{\gamma^2 D_{\mathcal{X}}^2 \rho \mathbf{C}_v}{1 - \rho} + \frac{\gamma D_{\mathcal{X}} D_0^y \mathbf{C}_1 \eta \rho^{k+2}}{\rho - \beta} + \frac{\gamma^2 D_{\mathcal{X}}^2 \mathbf{L}_y \mathbf{C}_1 \beta \eta}{(1 - \beta)(1 - \rho)} \right] + \frac{1}{2} \mathbf{L}_\ell \gamma^2 D_{\mathcal{X}}^2. \end{aligned} \quad (35)$$

Subtracting $\ell(\mathbf{x}^*)$ from both sides, we get

$$\ell(\mathbf{x}_{k+1}) - \ell(\mathbf{x}^*) \leq (1 - \gamma)(\ell(\mathbf{x}_k) - \ell(\mathbf{x}^*)) + \mathcal{R}_k(\gamma), \quad (36)$$

where

$$\begin{aligned} \mathcal{R}_k(\gamma) \triangleq & \gamma \mathbf{C}_2 \beta^k D_0^y D_{\mathcal{X}} + \frac{\gamma^2 \mathbf{C}_2 D_{\mathcal{X}}^2 \mathbf{L}_y \beta}{1 - \beta} + C_{yx}^g \left[\gamma D_{\mathcal{X}} \rho^{k+1} \|\mathbf{w}_0 - \mathbf{v}(\mathbf{x}_0)\| \right. \\ & \left. + \frac{\gamma^2 D_{\mathcal{X}}^2 \rho \mathbf{C}_v}{1 - \rho} + \frac{\gamma D_{\mathcal{X}} D_0^y \mathbf{C}_1 \eta \rho^{k+2}}{\rho - \beta} + \frac{\gamma^2 D_{\mathcal{X}}^2 \mathbf{L}_y \mathbf{C}_1 \beta \eta}{(1 - \beta)(1 - \rho)} \right] + \frac{1}{2} \mathbf{L}_\ell \gamma^2 D_{\mathcal{X}}^2. \end{aligned} \quad (37)$$

Continuing (36) recursively leads to the desired result. \square

D Proof of Corollary 4.3

We start the proof by using the result of the Theorem 4.3, i.e.,

$$\ell(\mathbf{x}_K) - \ell(\mathbf{x}^*) \leq (1 - \gamma)^K (\ell(\mathbf{x}_0) - \ell(\mathbf{x}^*)) + \sum_{k=0}^{K-1} (1 - \gamma)^{K-k} \mathcal{R}_k(\gamma). \quad (38)$$

Note that

$$\begin{aligned}
& \sum_{k=0}^{K-1} (1-\gamma)^{K-k} \mathcal{R}_k(\gamma) \\
&= \mathbf{C}_2 D_0^y D_{\mathcal{X}} \left[\sum_{k=0}^{K-1} (1-\gamma)^{K-k} \gamma \beta^k \right] + \frac{\mathbf{C}_2 D_{\mathcal{X}}^2 \mathbf{L}_y \beta}{1-\beta} \left[\sum_{k=0}^{K-1} (1-\gamma)^{K-k} \gamma^2 \right] \\
&\quad + C_{yx}^g \left(\rho D_{\mathcal{X}} \|\mathbf{w}_0 - \mathbf{v}(\mathbf{x}_0)\| \left[\sum_{k=0}^{K-1} (1-\gamma)^{K-k} \gamma \rho^k \right] + \frac{D_{\mathcal{X}}^2 \rho \mathbf{C}_v}{1-\rho} \left[\sum_{k=0}^{K-1} (1-\gamma)^{K-k} \gamma^2 \right] \right) \\
&\quad + \frac{D_{\mathcal{X}} D_0^y \mathbf{C}_1 \eta \rho^2}{\rho - \beta} \left[\sum_{k=0}^{K-1} (1-\gamma)^{K-k} \gamma \rho^k \right] + \frac{D_{\mathcal{X}}^2 \mathbf{L}_y \mathbf{C}_1 \beta \eta}{(1-\beta)(1-\rho)} \left[\sum_{k=0}^{K-1} (1-\gamma)^{K-k} \gamma^2 \right] \\
&\quad + \frac{1}{2} \mathbf{L}_\ell D_{\mathcal{X}}^2 \left[\sum_{k=0}^{K-1} (1-\gamma)^{K-k} \gamma^2 \right].
\end{aligned}$$

Moreover, one can easily verify that $\sum_{k=0}^{K-1} (1-\gamma)^{K-k} \gamma^2 \leq \gamma(1-\gamma)$ and $\sum_{k=0}^{K-1} (1-\gamma)^{K-k} \gamma \rho^k \leq \frac{\gamma(1-\gamma)}{|1-\gamma-\rho|}$ from which together with the above inequality we conclude that

$$\begin{aligned}
& \sum_{k=0}^{K-1} (1-\gamma)^{K-k} \mathcal{R}_k(\gamma) \\
&\leq \frac{\mathbf{C}_2 D_0^y D_{\mathcal{X}} \gamma (1-\gamma)}{|1-\gamma-\beta|} + \frac{\mathbf{C}_2 D_{\mathcal{X}}^2 \mathbf{L}_y \beta \gamma (1-\gamma)}{1-\beta} + C_{yx}^g \left(\frac{D_{\mathcal{X}} \rho \gamma (1-\gamma)}{|1-\gamma-\rho|} \|\mathbf{w}_0 - \mathbf{v}(\mathbf{x}_0)\| \right. \\
&\quad \left. + \frac{D_{\mathcal{X}}^2 \mathbf{C}_v \rho \gamma (1-\gamma)}{1-\rho} + \frac{D_{\mathcal{X}} D_0^y \mathbf{C}_1 \eta \rho^2 \gamma (1-\gamma)}{(\rho-\beta)|1-\gamma-\rho|} + \frac{D_{\mathcal{X}}^2 \mathbf{L}_y \mathbf{C}_1 \beta \gamma (1-\gamma)}{(1-\beta)(1-\rho)} \right) + \frac{1}{2} \mathbf{L}_\ell D_{\mathcal{X}}^2 \gamma (1-\gamma) \\
&= \mathcal{O} \left(\frac{\mathbf{C}_v \rho}{1-\rho} \gamma + \frac{\mathbf{L}_y \mathbf{C}_1 \beta}{(1-\beta)(1-\rho)} \gamma \right). \tag{39}
\end{aligned}$$

Using the above inequality within (38) we conclude that $\ell(\mathbf{x}_K) - \ell(\mathbf{x}^*) \leq (1-\gamma)^K (\ell(\mathbf{x}_0) - \ell(\mathbf{x}^*)) + \mathcal{O}(\frac{\mathbf{C}_v \rho}{1-\rho} \gamma + \frac{\mathbf{L}_y \mathbf{C}_1 \beta}{(1-\beta)(1-\rho)} \gamma)$ where $\mathbf{C}_v = \mathcal{O}(\kappa_g^3)$, $\mathbf{C}_1 = \mathcal{O}(\kappa_g^2)$, $\mathbf{L}_y = \mathcal{O}(\kappa_g)$ as shown in Lemma A.1 and $\min\{1-\rho, 1-\beta\} = \Omega(\frac{1}{\kappa_g})$ as shown in Lemma 4.1. Next, we show that by selecting $\gamma = \log(K)/K$ we have that $(1-\gamma)^K \leq 1/K$. In fact, for any $x > 0$, $\log(x) \geq 1 - \frac{1}{x}$ which implies that $\log(\frac{1}{1-\gamma}) \geq \gamma = \log(K)/K$, hence, $(\frac{1}{1-\gamma})^K \geq K$. Putting the pieces together we conclude that $\ell(\mathbf{x}_K) - \ell(\mathbf{x}^*) = \mathcal{O}((1-\gamma)^K (\ell(\mathbf{x}_0) - \ell(\mathbf{x}^*)) + \gamma \kappa_g^5) = \tilde{\mathcal{O}}(\kappa_g^5/K)$, which leads to an iteration complexity of $\tilde{\mathcal{O}}(\kappa_g^5 \epsilon^{-1})$.

Furthermore, assuming that $\nabla_y f(\mathbf{x}, \cdot)$ is uniformly bounded for any $\mathbf{x} \in \mathcal{X}$, we conclude that $C_y^f = \mathcal{O}(1)$, hence, $\mathbf{C}_1 = \mathcal{O}(\kappa_g)$ from which we have that $\ell(\mathbf{x}_K) - \ell(\mathbf{x}^*) = \mathcal{O}((1-\gamma)^K (\ell(\mathbf{x}_0) - \ell(\mathbf{x}^*)) + \gamma \kappa_g^4)$. Therefore, selecting $\gamma = \log(K)/K$ implies that $\ell(\mathbf{x}_K) - \ell(\mathbf{x}^*) = \mathcal{O}(\kappa_g^4/K)$ which leads to an iteration complexity of $\mathcal{O}(\kappa_g^4 \epsilon^{-1})$. \square

E Proof of Theorem 4.4

Recall that from Lemma B.4 we have

$$\begin{aligned} \mathcal{G}(\mathbf{x}_k) \leq & \frac{\ell(\mathbf{x}_k) - \ell(\mathbf{x}_{k+1})}{\gamma} + \mathbf{C}_2 \beta^k D_0^y D_{\mathcal{X}} + \frac{\gamma \mathbf{C}_2 D_{\mathcal{X}}^2 \mathbf{L}_y \beta}{1 - \beta} + C_{yx}^g \left[D_{\mathcal{X}} \rho^{k+1} \|\mathbf{w}_0 - \mathbf{v}(\mathbf{x}_0)\| \right. \\ & \left. + \frac{\gamma D_{\mathcal{X}}^2 \rho \mathbf{C}_v}{1 - \rho} + \frac{D_{\mathcal{X}} D_0^y \mathbf{C}_1 \eta \rho^{k+2}}{\rho - \beta} + \frac{\gamma D_{\mathcal{X}}^2 \mathbf{L}_y \mathbf{C}_1 \beta \eta}{(1 - \beta)(1 - \rho)} \right] + \frac{1}{2} \mathbf{L} \ell \gamma D_{\mathcal{X}}^2. \end{aligned}$$

Summing both sides of the above inequality from $k = 0$ to $K - 1$, we get

$$\begin{aligned} \sum_{k=0}^{K-1} \mathcal{G}(\mathbf{x}_k) \leq & \frac{\ell(\mathbf{x}_0) - \ell(\mathbf{x}_K)}{\gamma} + \frac{\mathbf{C}_2 D_0^y D_{\mathcal{X}}}{1 - \beta} + K \frac{\gamma \mathbf{C}_2 D_{\mathcal{X}}^2 \mathbf{L}_y \beta}{1 - \beta} + C_{yx}^g \left[\frac{\rho D_{\mathcal{X}} \|\mathbf{w}_0 - \mathbf{v}(\mathbf{x}_0)\|}{1 - \rho} \right. \\ & \left. + K \frac{\gamma D_{\mathcal{X}}^2 \rho \mathbf{C}_v}{1 - \rho} + \frac{D_{\mathcal{X}} D_0^y \mathbf{C}_1 \eta \rho^2}{(1 - \rho)(\rho - \beta)} + K \frac{\gamma D_{\mathcal{X}}^2 \mathbf{L}_y \mathbf{C}_1 \beta \eta}{(1 - \beta)(1 - \rho)} \right] + \frac{K}{2} \mathbf{L} \ell \gamma D_{\mathcal{X}}^2, \end{aligned}$$

where in the above inequality we use the fact that $\sum_{i=0}^{K-1} \beta^i \leq \frac{1}{1-\beta}$. Next, dividing both sides of the above inequality by K and denoting the smallest gap function over the iterations from $k = 0$ to $K - 1$, i.e.,

$$\mathcal{G}_{k^*} \triangleq \min_{0 \leq k \leq K-1} \mathcal{G}(\mathbf{x}_k) \leq \frac{1}{K} \sum_{k=0}^{K-1} \mathcal{G}(\mathbf{x}_k),$$

imply that

$$\begin{aligned} \mathcal{G}_{k^*} \leq & \frac{\ell(\mathbf{x}_0) - \ell(\mathbf{x}_K)}{K\gamma} + \frac{\gamma \mathbf{C}_2 D_{\mathcal{X}} \mathbf{L}_y \beta}{1 - \beta} + \frac{\gamma D_{\mathcal{X}}^2 \rho \mathbf{C}_v C_{yx}^g \rho}{1 - \rho} + \frac{\gamma D_{\mathcal{X}}^2 C_{yx}^g \mathbf{L}_y \mathbf{C}_1 \beta \eta}{(1 - \beta)(1 - \rho)} + \frac{1}{2} \mathbf{L} \ell \gamma D_{\mathcal{X}}^2 \\ & + \frac{\mathbf{C}_2 D_0^y D_{\mathcal{X}} \beta}{K(1 - \beta)} + \frac{D_{\mathcal{X}} C_{yx}^g \rho \|\mathbf{w}_0 - \mathbf{v}(\mathbf{x}_0)\|}{K(1 - \rho)} + \frac{D_{\mathcal{X}} D_0^y C_{yx}^g \mathbf{C}_1 \eta \rho^2}{K(\rho - \beta)(1 - \rho)}. \end{aligned} \quad (40)$$

□

F Proof of Corollary 4.5

We begin the proof by using the result of the Theorem 4.4.

$$\begin{aligned} \mathcal{G}_{k^*} \leq & \frac{\ell(\mathbf{x}_0) - \ell(\mathbf{x}_K)}{K\gamma} + \frac{\gamma \mathbf{C}_2 D_{\mathcal{X}} \mathbf{L}_y \beta}{1 - \beta} + \frac{\gamma D_{\mathcal{X}}^2 \rho \mathbf{C}_v C_{yx}^g \rho}{1 - \rho} + \frac{\gamma D_{\mathcal{X}}^2 C_{yx}^g \mathbf{L}_y \mathbf{C}_1 \beta \eta}{(1 - \beta)(1 - \rho)} + \frac{1}{2} \mathbf{L} \ell \gamma D_{\mathcal{X}}^2 \\ & + \frac{\mathbf{C}_2 D_0^y D_{\mathcal{X}} \beta}{K(1 - \beta)} + \frac{D_{\mathcal{X}} C_{yx}^g \rho \|\mathbf{w}_0 - \mathbf{v}(\mathbf{x}_0)\|}{K(1 - \rho)} + \frac{D_{\mathcal{X}} D_0^y C_{yx}^g \mathbf{C}_1 \eta \rho^2}{K(1 - \beta)(1 - \rho)} \\ = & \mathcal{O} \left(\frac{1}{K\gamma} + \frac{\gamma \mathbf{C}_2 \mathbf{L}_y \beta}{1 - \beta} + \frac{\gamma \mathbf{L}_y \mathbf{C}_1 \beta}{(1 - \beta)(1 - \rho)} \right) \end{aligned}$$

The desired result follows immediately from (40) and the fact that $\ell(\mathbf{x}^*) \leq \ell(\mathbf{x}_K)$. Moreover, similar to the proof of Corollary 4.3 we have that $\mathbf{C}_v = \mathcal{O}(\kappa_g^3)$, $\mathbf{C}_1 = \mathcal{O}(\kappa_g^2)$, $\mathbf{L}_y = \mathcal{O}(\kappa_g)$, and $\min\{1 - \rho, 1 - \beta\} = \Omega(\frac{1}{\kappa_g})$. Hence, by choosing $\gamma = 1/(\kappa_g^{2.5} \sqrt{K})$, we obtain that $\mathcal{G}_{k^*} = \mathcal{O}(\frac{1}{K\gamma} + \gamma \kappa_g^5) = \mathcal{O}(\kappa_g^{2.5}/\sqrt{K})$, which leads to an iteration complexity of $\mathcal{O}(\kappa_g^5 \epsilon^{-2})$.

Furthermore, assuming that $\nabla_y f(x, y)$ is uniformly bounded, we conclude that $C_y^f = \mathcal{O}(1)$, hence, $\mathbf{C}_1 = \mathcal{O}(\kappa_g)$ from which we have that $\mathcal{G}_{k^*} = \mathcal{O}(\frac{1}{K\gamma} + \gamma \kappa_g^4)$. Therefore, selecting $\gamma = 1/(\kappa_g^2 \sqrt{K})$ implies that $\mathcal{G}_{k^*} = \mathcal{O}(\kappa_g^2/\sqrt{K})$ which leads to an iteration complexity of $\mathcal{O}(\kappa_g^4 \epsilon^{-2})$. □

G Additional Experiments

In this section, we provide more details about the experiments conducted in section 5 as well as some additional experiments.

G.1 Experiment Details

In this section, we include more details of the numerical experiments in Section 5. The MATLAB code is also included in the supplementary material.

For completeness, we briefly review the update rules of SBFW Akhtar, Bedi, Thomdapu, and Rajawat [ABTR22] and TTSA Hong, Wai, Wang, and Yang [HWWY20] for the setting considered in problem (1). In the following, we use $\mathcal{P}_{\mathcal{X}}(\cdot)$ to denote the Euclidean projection onto the set \mathcal{X} .

Each iteration of SBFW has the following updates:

$$\begin{aligned}\mathbf{y}_k &= \mathbf{y}_{k-1} - \delta_k \nabla_y g(\mathbf{x}_{k-1}, \mathbf{y}_{k-1}), \\ \mathbf{d}_k &= (1 - \rho_k)(\mathbf{d}_{k-1} - h(\mathbf{x}_{k-1}, \mathbf{y}_{k-1})) + h(\mathbf{x}_k, \mathbf{y}_k), \\ \mathbf{s}_k &= \underset{\mathbf{s} \in \mathcal{X}}{\operatorname{argmin}} \langle \mathbf{s}, \mathbf{d}_k \rangle, \\ \mathbf{x}_{k+1} &= (1 - \eta_k)\mathbf{x}_k + \eta_k \mathbf{s}_k\end{aligned}$$

Based on the theoretical analysis in Akhtar, Bedi, Thomdapu, and Rajawat [ABTR22], $\rho_k = \frac{2}{k^{1/2}}$, $\eta_k = \frac{2}{(k+1)^{3/4}}$, and $\delta_k = \frac{a_0}{k^{1/2}}$ where $a_0 = \min \left\{ \frac{2}{3\mu_g}, \frac{\mu_g}{2L_y^2} \right\}$. Moreover, $h(\mathbf{x}_k, \mathbf{y}_k)$ is a biased estimator of the surrogate $\ell(\mathbf{x}_k)$ which can be computed as follows

$$h(\mathbf{x}_k, \mathbf{y}_k) = \nabla_x f(\mathbf{x}_k, \mathbf{y}_k) - M(\mathbf{x}_k, \mathbf{y}_k) \nabla_y f(\mathbf{x}_k, \mathbf{y}_k),$$

where the term $M(\mathbf{x}_k, \mathbf{y}_k)$ is a biased estimation of $[\nabla_{yy}^2 g(\mathbf{x}_k, \mathbf{y}_k)]^{-1}$ with bounded variance whose explicit form is

$$M(\mathbf{x}_k, \mathbf{y}_k) = \nabla_{yx}^2 g(\mathbf{x}_k, \mathbf{y}_k) \times \left[\frac{k}{L_g} \prod_{i=1}^l \left(I - \frac{1}{L_g} \nabla_{yy}^2 g(\mathbf{x}_k, \mathbf{y}_k) \right) \right],$$

and $l \in \{1, \dots, k\}$ is an integer selected uniformly at random.

The steps of TTSA algorithm are given by

$$\begin{aligned}\mathbf{y}_{k+1} &= \mathbf{y}_k - \beta h_k^g, \\ \mathbf{x}_{k+1} &= \mathcal{P}_{\mathcal{X}}(\mathbf{x}_k - \alpha h_k^f), \\ h_k^g &= \nabla_y g(\mathbf{x}_k, \mathbf{y}_k), \\ h_k^f &= \nabla_x f(\mathbf{x}_k, \mathbf{y}_k) - \nabla_{yx}^2 g(\mathbf{x}_k, \mathbf{y}_k) \times \left[\frac{t_{max}(k)c_h}{L_g} \prod_{i=1}^p \left(I - \frac{c_h}{L_g} \nabla_{yy}^2 g(\mathbf{x}_k, \mathbf{y}_k) \right) \right] \nabla_y f(\mathbf{x}_k, \mathbf{y}_k),\end{aligned}$$

where based on the theory we define $L = L_x^f + \frac{L_y^f C_{yx}^g}{\mu_g} + C_y^f \left(\frac{L_{yx}^g}{\mu_g} + \frac{L_{yy}^g C_{yx}^g}{\mu_g^2} \right)$, and $L_y = \frac{C_{yx}^g}{\mu_g}$, then set $\alpha = \min \left\{ \frac{\mu_g^2}{8L_y L L_y^2}, \frac{1}{4L_y L} K^{-3/5} \right\}$, $\beta = \min \left\{ \frac{\mu_g}{L_y^2}, \frac{2}{\mu_g} K^{-2/5} \right\}$, $t_{max}(k) = \frac{L_g}{\mu_g} \log(k+1)$, $p \in \{0, \dots, t_{max}(k) - 1\}$, and $c_h \in (0, 1]$.

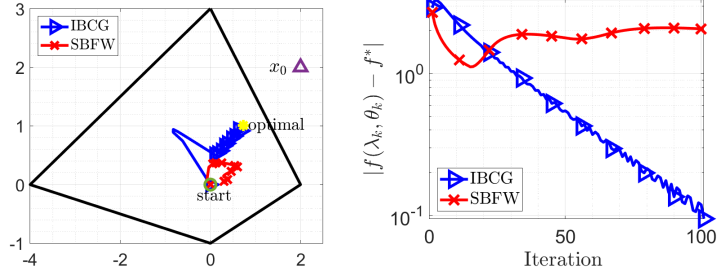


Figure 5: The performance of IBCG (blue) vs SBFW (red) on Problem (41) when $\mu_g = 1$. Plots from left to right are trajectories of θ_k and $f(\lambda_k, \theta_k) - f^*$.

G.2 Toy Example

Here we consider a variation of coreset problem in a two-dimensional space to illustrate the numerical stability of our proposed method. Given a point $x_0 \in \mathbb{R}^2$, the goal is to find the closest point to x_0 such that under a linear map it lies within the convex hull of given points $\{x_1, x_2, x_3, x_4\} \subset \mathbb{R}^2$. Let $A \in \mathbb{R}^{2 \times 2}$ represents the linear map, $X \triangleq [x_1, x_2, x_3, x_4] \in \mathbb{R}^{2 \times 4}$, and $\Delta_4 \triangleq \{\lambda \in \mathbb{R}^4 | \langle \lambda, \mathbf{1} \rangle = 1, \lambda \geq 0\}$ be the standard simplex set. This problem can be formulated as the following bilevel optimization problem

$$\min_{\lambda \in \Delta_4} \frac{1}{2} \|\theta(\lambda) - x_0\|^2 \quad \text{s.t.} \quad \theta(\lambda) \in \underset{\theta \in \mathbb{R}^2}{\operatorname{argmin}} \frac{1}{2} \|A\theta - X\lambda\|^2. \quad (41)$$

We set the target $x_0 = (2, 2)$ and choose starting points as $\theta_0 = (0, 0)$ and $\lambda_0 = \mathbf{1}_4/4$. We implemented our proposed method and compared it with SBFW [ABTR22]. It should be noted that in the SBFW method, they used a biased estimation for $[\nabla_{yy}^2 g(\lambda, \theta)]^{-1} = (A^\top A)^{-1}$ whose bias is upper bounded by $\frac{2}{\mu_g}$ (see Lemma 3.2 in [GW18]). Figure 5 illustrates the iteration trajectories of both methods for $\mu_g = 1$ and $K = 10^2$. The step-sizes for both methods are selected as suggested by their theoretical analysis. We observe that our method converges to the optimal solution while SBFW fails to converge. This situation for SBFW exacerbates for smaller values of μ_g .

Fig. 6 illustrates the iteration trajectories of both methods for $\mu_g = 0.1$ and $K = 10^3$ in which we also included SBFW method whose Hessian inverse matrix is explicitly provided in the algorithm. The step-sizes for both methods are selected as suggested by their theoretical analysis. Despite incorporating the Hessian inverse matrix in the SBFW method, the algorithm's effectiveness is compromised by excessively conservative step-sizes, as dictated by the theoretical result. Consequently, the algorithm fails to converge to the optimal point effectively. Regarding this issue, we tune their step-sizes, i.e., scale the parameter δ and η in their method by a factor of 5 and 0.1, respectively. By tuning the parameters we can see in Fig. 7 that the SBFW with Hessian inverse matrix algorithm has a better performance and converges to the optimal solution. In fact, using the Hessian inverse as well as tuning the step-sizes their method converges to the optimal solution while our method always shows a consistent and robust behavior.

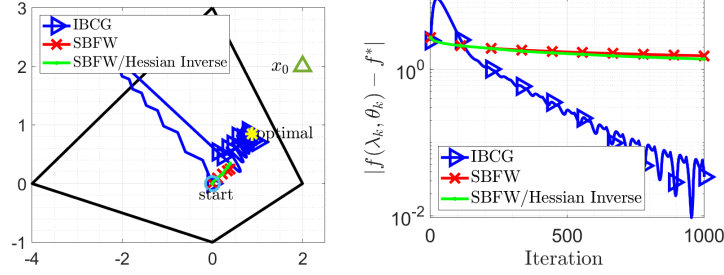


Figure 6: The performance of IBCG (blue) vs SBFW (red) and SBFW with Hessian inverse (green) on Problem (41) when $\mu_g = 0.1$. Plots from left to right are trajectories of θ_k and $f(\lambda_k, \theta_k) - f^*$.

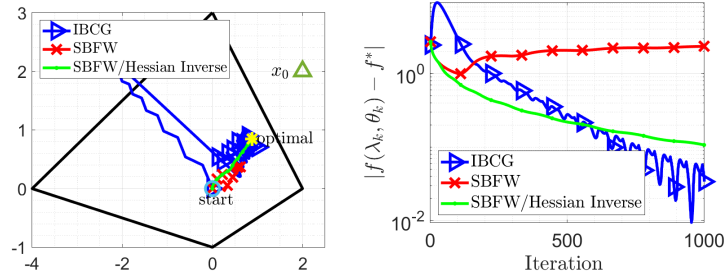


Figure 7: The performance of IBCG (blue) vs SBFW (red) and SBFW with Hessian inverse (green) on Problem (41) when $\mu_g = 0.1$ and the SBFW parameters are tuned. Plots from left to right are trajectories of θ_k and $f(\lambda_k, \theta_k) - f^*$.

G.3 Matrix Completion with Denoising

G.3.1 Synthetic dataset

Dataset Generation. We create an observation matrix $M = \hat{X} + E$. In this setting $\hat{X} = WW^T$ where $W \in \mathbb{R}^{n \times r}$ containing normally distributed independent entries, and $E = \hat{n}(L + L^T)$ is a noise matrix where $L \in \mathbb{R}^{n \times n}$ containing normally distributed independent entries and $\hat{n} \in (0, 1)$ is the noise factor. During the simulation process, we set $n = 250$, $r = 10$, and $\alpha = \|\hat{X}\|_*$.

Initialization. All the methods start from the same initial point \mathbf{x}_0 and \mathbf{y}_0 which are generated randomly. We terminate the algorithms either when the maximum number of iterations $K_{\max} = 10^4$ or the maximum time limit $T_{\max} = 2 \times 10^2$ seconds are achieved.

Implementation Details. For our method IBCG, we choose the step-sizes as $\gamma = \frac{1}{4\sqrt{K}}$ to avoid instability due to large initial step-sizes, and set $\alpha = 2/(\mu_g + L_g)$ and $\eta = 0.9 \times \frac{1-\beta}{\mu_g}$. We tuned the step-size η_k in the SBFW method by multiplying it by a factor of 0.8, and for the TTSA method, we tuned their step-size β by multiplying it by a factor of 0.25.

G.3.2 Real dataset

In order to emphasize the importance of projection-free bilevel algorithms in practical applications, we conducted further experiments using a larger dataset known as MovieLens 1M. This dataset consists of 1 million ratings provided by 6000 individuals for a total of 4000 movies. In Figure 8 the inferior performance of TTSA algorithm in actual computation time, especially when dealing with

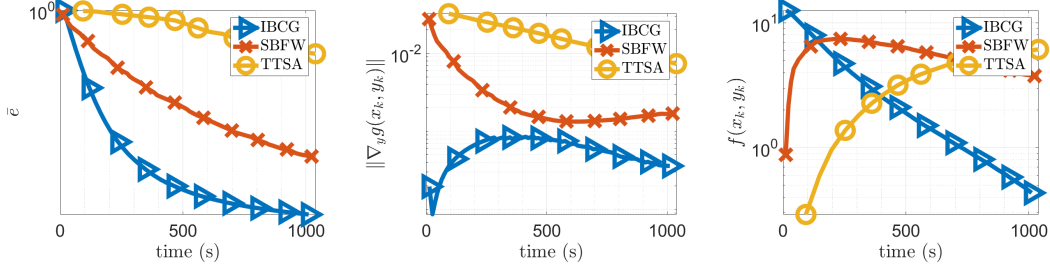


Figure 8: The performance of IBCG (blue) vs SBFW (red) and TTSA (yellow) on Problem (2) for real dataset. Plots from left to right are trajectories of normalized error ($\bar{\epsilon}$), $\|\nabla_y g(\mathbf{x}_k, \mathbf{y}_k)\|$, and $f(\mathbf{x}_k, \mathbf{y}_k)$ over time.

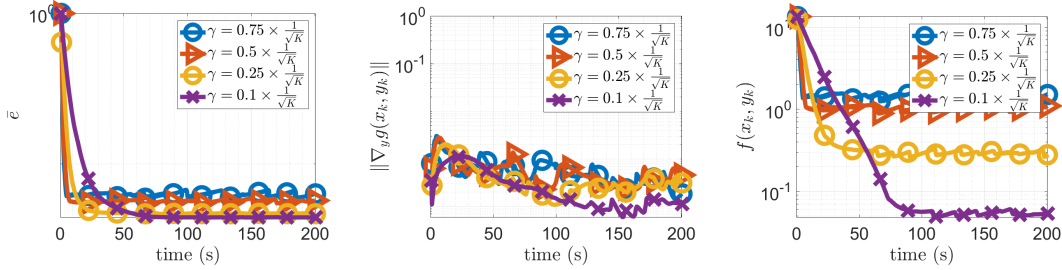


Figure 9: The performance of IBCG on Problem (2) for fixed step-sizes η and α . Plots from left to right are trajectories of normalized error ($\bar{\epsilon}$), $\|\nabla_y g(\mathbf{x}_k, \mathbf{y}_k)\|$, and $f(\mathbf{x}_k, \mathbf{y}_k)$ over time.

large datasets becomes more evident. The observed difference can be attributed to the utilization of the projection operation in contrast to the projection-free algorithms. TTSA requires performing projections over nuclear norm at each iteration which is computationally expensive due to the computation of full singular value decomposition. In contrast, projection-free algorithms IBCG and SBFW solve a linear minimization at each iteration, which only requires the computation of singular vectors corresponding to the largest singular value. On the other hand, considering the slow convergence rate of SBFW, when the size of the dataset increases, the improved performance of our proposed method becomes more evident compared to SBFW.

Moreover, in the following, we utilized the MovieLens 100k dataset to implement matrix completion with denoising examples for different step-sizes. These experiments will be designed to explore how different step-size selections impact the performance of the IBCG algorithm. We fix the step-sizes $\alpha = 2/(\mu_g + L_g)$ and $\eta = 0.5 \times \frac{1-\beta}{\mu_g}$ and systematically alter $\gamma = c_1 \times \frac{1}{\sqrt{K}}$ with constants $c_1 \in \{0.75, 0.5, 0.25, 0.1\}$ as depicted in Fig. 9. We observe that larger values of γ directly affect the performance of the algorithm. This observation matches with our theoretical result as demonstrated in Lemma B.3. In particular, the error of approximating the lower-level solution and its Jacobian is directly related to the step-size γ and larger values of γ contributing to larger errors affecting the upper-level objective value.

In Fig. 10, we fixed the step-sizes $\alpha = 2/(\mu_g + L_g)$ and $\gamma = 0.1 \times \frac{1}{\sqrt{K}}$ and changed the value of step-size $\eta = c_2 \times \frac{1-\beta}{\mu_g}$ with constants $c_2 \in \{0.75, 0.5, 0.25, 0.1\}$. The performance of the IBCG is robust due to the various values of step-size η . This indicates that the choice of η does not significantly affect the convergence rate, suggesting that the IBCG method is not overly sensitive to this parameter within the tested range. The algorithm achieves comparable accuracy levels in the end, regardless of the initial choice of c_2 , signifying a level of stability that can be beneficial in

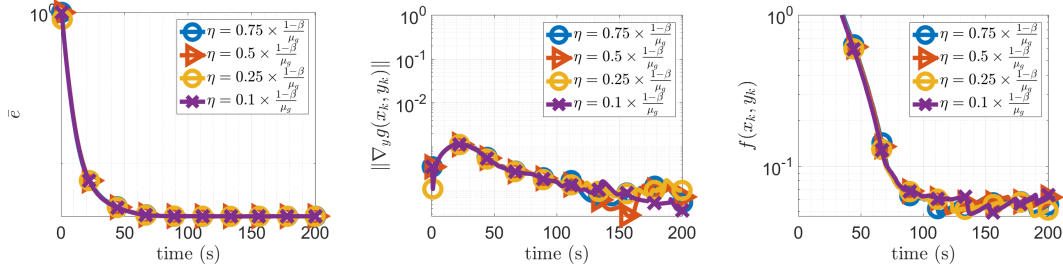


Figure 10: The performance of IBCG on Problem (2) for fixed step-sizes γ and α . Plots from left to right are trajectories of normalized error (\hat{e}), $\|\nabla_y g(\mathbf{x}_k, \mathbf{y}_k)\|$, and $f(\mathbf{x}_k, \mathbf{y}_k)$ over time.

Model	Dataset1					Average
	bodyfat	housing	mg	mpg	space-ga	
Individual regression	0.1771	7.6547	0.6333	1.7412	0.5232	2.1459
MTL_IBCG	0.0599	1.1630	0.0480	3.2205	0.0245	0.9032
MTL_SBFW	0.0783	0.9675	0.0540	3.4654	0.0253	0.9181

Table 2: Test error of applying Ridge regression on each dataset vs test error of IBCG and SBFW methods for multi-task learning problem presented in (3)

practical applications where the optimal step-size may not be known at first.

G.4 Multi-Task Learning

Dataset 1. In this experiment, we consider a collection of datasets: `bodyfat`, `housing`, `mg`, `mpg`, and `space-ga` from LibSVM library [CL11]. We consider each dataset as distinct data points for each task. To standardize the feature space across these datasets, we extend the number of features in each by adding columns of zeros to the datasets that originally had fewer features. Furthermore, all datasets are scaled to fit within the range of $[-1, 1]$.

Initialization. For both methods we choose $\lambda_1 = \lambda_2 = 0.1$ and start from the same initial point Ω_0 and W_0 . We terminate the algorithms either when the maximum number of iterations $K_{\max} = 10^4$ or the maximum time limit $T_{\max} = 100$ seconds are achieved.

Implementation Details. For our method IBCG, we choose the step-sizes as $\gamma = \frac{1}{10^4 \times \sqrt{K}}$, and set $\eta = 0.9 \times \frac{1-\beta}{\mu_g}$. We tuned the step-sizes η_k, γ_k, ρ_k in the SBFW method by multiplying all by a factor of 10^3 . Moreover, we scale the parameter a_0 by multiplying it by a factor of 100. Empirically, we observe that these modifications lead to faster convergence in SBFW.

Furthermore, we compare the performance of the MTL model considered in (3) over the test dataset after training with IBCG and SBFW algorithms and compared with the performance of each dataset individually trained by a ridge regression (RR) model. The results of the test error are depicted in Table 2. The considered bilevel MTL model improves the test accuracy for 4 out of 5 datasets considered. In fact, the average test error of RR models is 2.1459 while our method achieves 0.9032. Moreover, comparing the performance of our proposed method with SBFW we observe that the test error for IBCG is lower in most of the datasets with an average of 0.9032 while SBFW leads to an average test error of 0.9181.

Dataset 2. We consider the 1979 National Longitudinal Survey of Youth (NLSY79)¹ dataset

¹NLSY79 Data Overview

Model	Dataset2										Average
	1	2	3	4	5	6	7	8	9	10	
Individual regression	5.620	5.852	14.358	2.993	6.910	13.590	14.463	2.444	3.804	2.993	7.3027
MTL-IBCG	1.2853	1.0021	1.1868	1.1131	1.4108	0.9580	1.1280	1.1849	1.3763	1.1845	1.1830
MTL-SBFW	1.7794	1.6111	1.8025	1.5937	1.9606	1.4405	1.7451	1.8579	2.0640	1.9039	1.7759

Table 3: Test error of applying Ridge regression on each dataset vs test error of IBCG and SBFW methods for multi-task learning problem presented in (3)

which consists of a data matrix $\mathbf{A} \in \mathbb{R}^{n \times d}$ with $n = 6213$ instances and $d = 19$ attributes and an outcome vector $\mathbf{b} \in \mathbb{R}^n$. We assign 60% of the dataset as the training set ($\mathbf{A}^{\text{tr}}, \mathbf{b}^{\text{tr}}$), 20% as the validation set ($\mathbf{A}^{\text{val}}, \mathbf{b}^{\text{val}}$) and the rest as the test set ($\mathbf{A}^{\text{test}}, \mathbf{b}^{\text{test}}$). To align the dataset with the structure of our problem, we partition the data matrix $\mathbf{A} \in \mathbb{R}^{n \times d}$ and the associated response vector $\mathbf{b} \in \mathbb{R}^n$ into $T = 10$ distinct segments. This ensures that each task is allocated n_i data points i.e $\mathbf{A}_i \in \mathbb{R}^{n_i \times d}, \mathbf{b}_i \in \mathbb{R}^{n_i}$, with the cumulative total across all tasks $\sum_{i=1}^T n_i$ equating to n .

Initialization. For both methods we choose $\lambda_1 = \lambda_2 = 0.1$ and start from the same initial point Ω_0 and W_0 . We terminate the algorithms either when the maximum number of iterations $K_{\text{max}} = 10^4$ or the maximum time limit $T_{\text{max}} = 100$ seconds are achieved.

Implementation Details. For our method IBCG, we choose the step-sizes as $\gamma = \frac{1}{10^{8 \times \sqrt{K}}}$ to avoid instability due to large initial step-sizes, and set $\alpha = \frac{2}{(\mu_g + L_g)}$ and $\eta = 0.9 \times \frac{1-\beta}{\mu_g}$. We tuned the step-sizes η_k, γ_k, ρ_k in the SBFW method by multiplying all by a factor of 100. Moreover, we scale the parameter a_0 by multiplying it by a factor of 10. Empirically, we observe that these modifications lead to a better performance of SBFW in terms of both gradient norm of the lower-level problem and upper-level objective function value.

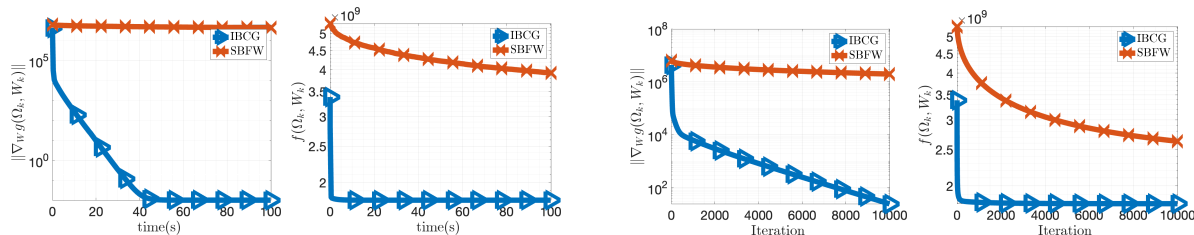


Figure 11: Performance of IBCG vs SBFW on problem (3) for real dataset2. Plots from left to right: $\|\nabla_{W_k} g(\Omega_k, W_k)\|$, and $f(\Omega_k, W_k)$ over time and fixed number of iterations, respectively.

The performance comparison between our IBCG method and the SBFW method for problem (3) on real dataset 2 is depicted in Fig. 11. In terms of lower-level gradient norm, IBCG shows a rapid initial decrease and then, indicates a fast convergence rate, however, SBFW exhibits a slower descent. The upper-level function value plots further corroborate these findings, with IBCG achieving a substantially lower function value quickly, demonstrating its superior performance.

Similar to the experiment for Dataset1, we compare the performance of the MTL model in (3) over the test dataset after training with IBCG and SBFW algorithms and compared with the performance of each partition individually trained by an RR model. The results of the test error are depicted in Table 3. The average test error of RR models is 7.3027 while our method achieves 1.1830. Moreover, comparing the performance of our proposed method with SBFW we observe that the test error for IBCG is lower in all of the datasets with an average of 1.1830 while SBFW leads to an average test error of 1.7759.